学位論文（要約）

Transcriptional regulation of gene expressions in middle wavelengths-sensitive cone photoreceptors of zebrafish

(ゼブラフィッシュにおいて中波長領域感受性を示す錐体の遺伝子発現制御)

平成28年12月博士（理学）申請

東京大学大学院理学系研究科
生物科学専攻

小川　洋平

Abstract

Color discrimination in vertebrates is mediated by a combination of multiple subtypes of cone photoreceptor cells in the retina. Previous studies have made considerable progress in understanding molecular mechanism underlying specification of cone subtypes governed by transcription factors. In spite of these advances, it remains elusive how to organize the development of cone subtypes for high-acuity color vision, prevalent in many diurnal vertebrates and is achieved by a set of four cone subtypes expressing UV-, blue-, green- and red-sensitive cone opsin genes. In particular, none of transcription factors was identified to be responsible for regulation of middle wavelength-sensitive cones, blue and green cones. Moreover, a role of middle wavelength-sensitive cones in the high-acuity color vision has not been investigated. In this study, I explored developmental mechanism of cone photoreceptors in zebrafish (*Danio rerio*), which has all the four cone subtypes and represents a valuable vertebrate model. I focused on the cone-enriched transcription factors determined by our previous microarray analysis of purified rod cells and cone cells. I generated several lines of knock-out zebrafish with TAL effector nucleases (TALENs), and examined an effect of the loss of the cone-enriched transcription factors on the expression of visual opsin genes by RT-qPCR, *in situ* hybridization and immunohistochemical analysis.

I found that *sine oculis homeobox homolog 7* (*six7*), a transcription factor widely conserved in ray-finned fish, is expressed predominantly in the zebrafish cone photoreceptors throughout retinal development. Genetic ablation of *six7* severely reduced the expression of all the green opsin genes at both the larval and adult stages, indicating that *six7* is essential for the expression of green opsin gene.

Contents

1. Introduction

In the animal kingdom, vision is one of the important sensory modalities for acquiring environmental information. In vertebrates, visual information is initially mediated by two types of photoreceptor cells: rods and cones. They are distinct from each other in morphology and photoresponse (1–3), and function under different light conditions; rods are responsible for twilight vision, while cones function under the daylight condition. The characteristic features of rods and cones are ensured by specific phototransduction component genes, and also by precise transcriptional regulation of these genes. Particularly, visual opsins, which are photoreceptive molecules and localized in outer segment of photoreceptors, are exclusively expressed in the rods or cones. In addition, most vertebrate species have multiple cone opsin genes, and they are exclusively expressed in one subtype of the cone photoreceptors. Diverged spectral sensitivities among the cone opsin genes confer cone subtypes with different wavelength-sensitivities, and thus a combination of multiple cone subtypes provides many vertebrates with color discrimination. In photic environment, chromatic information is useful for their survival.

High-acuity color vision is achieved by a combination of UV-, blue-, green- and red-sensitive cones (4, 5). Four types of cone opsin genes, namely, UV (short wavelength sensitive 1: SWS1), blue (short wavelength sensitive 2: SWS2), green (medium wavelength sensitive: RH2) and red (long wavelength sensitive: M/LWS) are exclusively expressed in the corresponding cone subtype. The high-acuity color vison is equipped in various vertebrate species such as fish, reptiles and birds [(6–8) and figure 1], and also in the southern hemisphere lamprey, *Geotria australis* (9). It is a jawless vertebrate whose ancestor diverged from a lineage leading to jawed vertebrates probably more than 500 Mya (10), and thus the tetrachromatic color vision system is thought to have been acquired before the agnathan/gnathostome split in the

vertebrate lineage (11). Tetrachromat benefit is suggested by recent study reporting reduced foraging activity by the loss of UV cones in zebrafish (*Danio rerio*) (12). On the other hand, physiological function of blue and green cones for the high-acuity color vision has not been investigated.

Molecular basis for development of visual photoreceptors have been well studied in mouse (*Mus musculus*), and many research groups have identified important transcription factors responsible for gene regulation of rod and cone opsins, and for development of the photoreceptors in mice (13–16). In particular, cone-rod homeobox (*Crx*) is a master transcriptional regulator for differentiation of retinal progenitor cells into photoreceptor cells (17–19). Further differentiation into rod photoreceptor requires additional expression of neural retina leucine zipper (*Nrl*) and nuclear receptor subfamily 2 group E member 3 (*Nr2e3*) (20, 21). The loss of *Nrl* compromises rod formation and causes an excess of cone photoreceptors expressing *SWS1* opsin genes, and over-expression of *Nrl* transforms most cone precursors into functional rods (22). *Nr2e3*, the expression of which is activated by *Nrl*, represses cone-specific genes in developing rods, thereby promoting the rod development (20). On the other hand, previous study in zebrafish reported that the loss of T-box 2b (*tbx2b*) increases the number of rods and reduces the number of cone photoreceptors expressing *SWS1* at the larval stage (23) and presented a reciprocal system for the rod vs. cone neurogenesis. However, it is not known whether the expression of rod specific genes is repressed by transcription factors during the development of the cone photoreceptors.

Molecular mechanisms underlying specification of the cone subtypes were also well studied in mice. In particular, thyroid hormone receptor beta (*Thrb*) specifies the cone subtype expressing *M/LWS* opsin gene in combination with *Crx*. *Thrb* activates and represses the expression of *M/LWS* and *SWS1* opsin genes, respectively (24–26). In spite of the increasing knowledge of cone photoreceptor development, for the high-acuity color vision, molecular basis underlying the specification of cone subtype

remains elusive especially for *SWS2* and *RH2* cone opsin genes. The loss of *SWS2* and *RH2* cone opsin genes in mammals makes it difficult to understand transcriptional mechanisms for development of the four cone subtypes (figure 1). Thus, the vertebrate species having all the four cone subtypes should be employed for revealing the transcriptional network underlying the high-acuity color vision system and for understanding relationships between alteration in the transcriptional network and diversity of cone subtypes during the evolution of vertebrates.

Zebrafish (*Danio rerio*) is a diurnal teleost with four cone subtypes (UV: *sws1*, blue: *sws2*, green: *rh2,* red: *lws*). Zebrafish is a valuable animal model to study molecular mechanisms of vertebrate retinal development and disease (27, 28), and also used for revealing the specification of the cone subtypes (figure 2). Similar to mouse, *crx* and its paralog orthodenticle homolog 5 (*otx5*) are also the master transcriptional regulators of photoreceptor cells in zebrafish (29, 30). T-box 2b (*tbx2b*) and thryroid hormone receptor beta (*thrb*) were identified to be essential for the expression of *sws1* (23) and *lws* (31), respectively. The regulation of *crx* and *thrb* was observed both in mouse and zebrafish. The conserved regulation of the cone opsin gene suggests that these two vertebrate species partly share a regulatory mechanism underlying the development of the cone photoreceptors. Despite these findings, none of transcription factors has been identified to be responsible for expression of *sws2* and *rh2* in vertebrates.

In addition to four types of cone opsin genes, tandem gene duplication results in emergence of additional cone opsin genes, often observed in teleost (32). For instance, zebrafish possesses variable number of duplicated green opsin genes (*rh2-1, rh2-2, rh2-3* and *rh2-4*) and red opsin genes (*lws1* and *lws2*, which also refer to as *lws1/2* in this study). The duplicated cone opsins were diverged in spectral sensitivities from each other (33) and their expression is spatio-temporally regulated in each cone subtype (34). Thus, these duplicated cone opsins are thought to contribute to teleost

adaptation of diverse aquatic environments. It still remains elusive whether and how the spatio-temporal regulation of the duplicated cone opsin genes is mediated by transcription factors.

To understand the development of cone photoreceptors and the gene regulation of cone opsin genes in zebrafish, I used our microarray data. Previously, we compared gene expression profiles between rod and cone cells purified from the adult zebrafish retina (Shiraki *et al.,* unpublished data). Among the cone-enriched genes, I found that *sine oculis homeobox homolog* 7 (*six7*) is predominantly expressed in cone photoreceptors. The Six family is a group of evolutionarily conserved transcription factors found in diverse organisms ranging from flies to humans (35–37). The first identified Six family gene is *Drosophila sine oculis* (*so*), an essential transcription factor for compound eye formation. In the vertebrate lineage, SIX genes are classified into three subfamilies: Six1/Six2, Six3/Six6/Six7 and Six4/Six5 subfamily (figure 3). Six1/Six2 and Six4/Six5 group members are involved in the development of non-eye issues such as skeletal muscles, limb buds, kidneys, noses and ears. On the other hand, Six3/Six6/Six7 group members play a role during eye and brain formation. Previous studies reported that the expression of *six7* is detected during gastrulation and early segmentation (38), and that the inactivation of *six7* and *six3b* causes the loss of the zebrafish eyes (39). Despite the engagement of *six7* in early eye development, it still remains unclear whether and how *six7* is involved in the development of cone photoreceptors. I investigated roles of *six7* in the regulation of cone development and cone opsin gene expression by generating *six7* knock-out zebrafish with TAL effector nucleases (TALENs). The *six7* knock-out severely reduced the expression of all the green opsin genes at both larval and adult stages, indicating that *six7* is indispensable for the development and/or maintenance of the green cones. Furthermore, the loss of *six7* caused switching of the expression of the red cone opsin genes from *lws2* to *lws1*, in the central retina at the adult stage, suggesting that *six7* engages in the spatio-

temporal expression of cone opsin genes. In contrast to the reduced expression of green opsin genes, the loss of *six7* increase the number of rod photoreceptors at the larval stage. In addition, photoreceptor-specific over-expression of *six7* significantly reduced the expression of rod-specific phototransduction genes, while the expression levels of cone opsin genes were unaffected by the over-expression of *six7*. Considering that *six7* is predominantly expressed in cone photoreceptors, the loss- and gain-of-function experiments suggest that *six7* repress the rod development in developing cones, and thereby promoting the cone development.

以下、5 年以内に雑誌等で刊行予定のため、非公開。

2. Materials and methods

(1) Zebrafish

All research described here adhered to local guidelines of the University of Tokyo and all appropriate ethical approval and licenses were obtained. The wild-type zebrafish (EkkWill strain) were raised in a 14-h light/10-h dark cycle, and fed twice per day with living baby brine shrimps. Embryos were raised at 28.5°C in egg water (artificial seawater diluted 1.5:1000 in water). For detection of EGFP expression in the eye of transgenic zebrafish, larvae were treated with fish water containing 0.003% 1-phenyl-2-thiourea (PTU) 24 hours after fertilization until 5 days post-fertilization to transiently block synthesis of melanin pigment

(2) Generation of mutant zebrafish

Construction of TALEN targeting-vector

For generation of pTAL7DD and pTAL7RR plasmid vectors, I amplified a sequence encoding the TAL effector and the *Fok*I nuclease catalytic domain from the pTAL3 (Addgene plasmid 31034) by PCR and cloned between *BamH*I and *EcoR*I site of pCS2(+) vector. Based on pCS2TAL3DD and pCS2TAL3RR vectors (40), the N-terminal and C-terminal regions of the TAL effector were truncated. The resulting vector pTAL7DR was further modified by PCR for generation of pTAL7RR and pTAL7DD, the nucleotide sequence of which is shown in our previous study (41). A pair of pTAL7DD and pTAL7RR express a DD-RR heterodimeric form of the catalytic domain of *Fok*I nuclease, and this form was previously shown to have reduced homodimeric cleavage activity, and thereby decreased toxicity of zinc finger nucleases (42).

Generation of *six7* mutant zebrafish

For generation of *six7* mutant, TAL effector repeats recognizing exon 1 of zebrafish *six7* gene were designed. These repeats were cloned into pTAL7DD and/or pTAL7RR. Construction of pTAL7DD and pTAL7RR vectors was described above. TALEN mRNA was synthesized from the pTAL7DD and pTAL7RR by *in vitro* transcription using the SP6 mMESSAGE mMACHINE Kit (AM13140, Ambion), and purified with the RNeasy Mini kit (74104, Qiagen). A pair of the TALEN mRNAs (~200 pg) in 0.05% phenol red were injected into the cytoplasm of the one cell-stage embryos. The injected fish (F_0) were raised and crossed with wild-type zebrafish, and the F_1 fish embryos with TALEN-induced mutations were isolated by PCR and subsequent digestion by endonuclease *Xho*I; first, the region surrounding the TALEN cleavage site was amplified by PCR using the primers, six7TALEN_Fw and six7TALEN_Rv (table 1). Second, the PCR product was digested by *Xho*I, and TALEN-induced mutations were examined by sensitivities to the *Xho*I digestion. To verify mutations, the PCR products having no *Xho*I site were then subjected to the second round of PCR using the other primers, DS_six7TALEN_Fw and DS_six7TALEN_Rv (table 1). The nested PCR products were digested by *Xho*I again, and then sequenced directly. For genotyping of *six7*^{ja51} mutant fish, PCR was performed with two pairs of specific primers, (i) DS_six7TALEN_Fw and DS_six7TALEN_Rv, (ii) six7TALEN_Fw2WT and six7TALEN_Rv3mut (table 1). For the experiments with the larval eyes of the mutant, the larvae were dissected into anterior and posterior segments; the posterior ones were used for the genotyping, while the anterior segments were soaked in RNA*later* (R0901, Sigma) for extracting RNA or soaked in 4% paraformaldehyde in Ca^{2+}- and Mg^{2+}-free Dulbecco's PBS (D-PBS) for preparing cryosections.

Generation of *six3b* mutant zebrafish

The *six3b* mutant zebrafish was generated in a similar manner to the *six7* mutant. Briefly, the F_1 fish were screened for the presence of TALEN-induced mutations by a combination of PCR and subsequent digestion by endonuclease *Hind*III. After isolating the mutant zebrafish and verifying the mutations in the *six3b* gene locus, genotypes were determined by a combination of PCR and subsequent digestion by endonuclease *Hind*III. First, the region flanking the TALEN cleavage site was amplified by PCR using the following primers, six3bTALEN_Fw and six3bTALEN_Rv (table 1). Second, the PCR product was digested with *Hind*III, and TALEN-induced mutations were checked by loss of the *Hind*III digestion site.

以下、5 年以内に雑誌等で刊行予定のため、非公開。

Table 1.

Primers used for genotyping of mutant zebrafish.

Primer Name	Primer sequence (5' to 3')
six7TALEN_Fw	TCTGCTGCTCCTCCTTTAC
six7TALEN_Rv	CTTACGGATGCGGTACTTC
DS_six7TALEN_Fw	CCGTTGGTTGTCCGTTACTC
DS_six7TALEN_Rv	GCAGTTTAGCGTGAGATTCG
six7TALEN_Fw2WT	CCCGAGTGTGCGAGAATC
six7TALEN_Rv3mut	GCTCGATATCTCCTGTTTTCC
six3bTALEN_Fw	GACACCAGGAAGACCAATAG
six3bTALEN_Rv	TACCACTCCCTCAACAAACC

以下、5 年以内に雑誌等で刊行予定のため、非公開。

(3) Immunohistochemistry

Immunohistochemistry with ocular sections

Fixing embryos and isolating the eye of adult zebrafish were performed under light condition for controlling the movement of pigment granules (43). After isolation of the adult eyes and removal of the lenses, the eyes were fixed in 4% paraformaldehyde (PFA) in Ca^{2+}- and Mg^{2+}-free Dulbecco's PBS (D-PBS) overnight at 4°C. The fixed eyes were washed several times with D-PBS, then soaked successively in 5%, 10% and 15% sucrose in D-PBS for 30 min each at room temperature and finally soaked in 20% sucrose in D-PBS overnight at 4°C. On the other hand, the embryos were fixed in 4% PFA in D-PBS overnight at 4°C. After washing twice with D-PBS and with 5% sucrose in D-PBS, the fixed samples were soaked in 20% sucrose in D-PBS overnight at 4°C. The cryoprotected samples of the adult eyes and embryos were infiltrated in a 2:1 solution of 20% sucrose in D-PBS and Tissue-Tek O.C.T Compound (Tissue-Tek, SAKURA) for 1-2 hr at room temperature. The treated samples were frozen and sectioned with cryostat (CM3000, Leica). The sections on the glass slides (10 μm thickness) were washed three times with PBS (10 mM Na-phosphate buffer, 140 mM NaCl, 1 mM $MgCl_2$, pH 7.4) for 10 min each, soaked with a blocking solution (3% goat normal serum, 0.1% Triton X-100 in PBS) for 1 hr at room temperature, and then incubated with a primary antibody diluted in the blocking solution overnight at 4°C. After washed three times with PBS for 10 min each, the samples were immersed with the blocking solution for 15 min at room temperature, and then incubated for 4 hr at room temperature with a secondary antibody or incubated with a secondary antibody and 3 μg/ml DAPI for staining of the cell nuclei. After washed three times with PBS for 10 min each, the sections were coverslipped with VECTASHIELD Mounting Medium with DAPI (Vector Laboratories) or VECTASHIELD Mounting Medium (Vector Laboratories). The primary antibodies used were as follows: mouse monoclonal antibody Zpr1 (diluted

1:400, Zebrafish International Resource Center, Eugene) against arrestin 3a, which is a specific cone phototransduction gene in double cones (green and red cones); rabbit polyclonal antibody against rod transducin α-subunit, Gnat1 (diluted to 0.5 μg/ml, sc-389, Santa Cruz); mouse polyclonal antibody to rhodopsin (diluted 1:400, self-produced antibody); rabbit polyclonal antibody to cone transducin α-subunit, Gnat2 (diluted 1:800, PM075, MBL). The secondary antibodies used were goat anti-mouse IgG antibody conjugated with Alexa-568 (diluted to 2 μg/ml, A-11004, Molecular Probes) and goat anti-rabbit IgG antibody conjugated with Alexa-488 (diluted to 2 μg/ml, A-11034, Molecular Probes). The coverslipped slides were observed with a confocal laser scanning microscope (TCS SP8, Leica) and/or with a microscope (BZ-9000 Generation II, Keyence).

Whole-mount immunohistochemistry

Whole-mount immunohistochemistry was performed as described previously (44) with some modifications. Under a dim red light condition, I enucleated the dark-adapted adult zebrafish and isolated the retinas. The isolated retinas were fixed in 4% PFA in D-PBS for 3 hr at 4°C. After washing three times with 0.1% Triton-X100 in PBS (PBST2) for 5 min each, the samples were incubated with 0.5% Triton-X100 in PBS for 30 min at room temperature, then washed twice with PBST2 for 5 min each. The treated samples were incubated in a blocking solution (2% goat normal serum, 1% Dimethyl sulfoxide in PBST2) for 1 hr at room temperature, and then with a primary antibody diluted in the blocking solution overnight at 4°C. After rinsing with PBST2 for 1 min and washing three times with PBST2 for 20 min each, the specimens were incubated with the blocking solution for 1 hr at room temperature, and then with a secondary antibody for 4 hr at room temperature. Washing four times with PBST2 for 20 min each, the incubated retinas were mounted on a grass slide and coverslipped with VECTASHIELD Mounting Medium with DAPI for staining of the cell nuclei. The

primary antibodies used were as follows: mouse monoclonal antibody 1D4 (45) (diluted to 7 μg/ml), which specifically recognized red cone opsins in zebrafish; rabbit polyclonal antibody to cone transducin α-subunit, Gnat2 (diluted 1:400, PM075, MBL). The secondary antibodies used were goat anti-mouse IgG antibody conjugated with Alexa-568 (A-11004, diluted to 4 μg/ml, Molecular Probes) and goat anti-rabbit IgG antibody conjugated with Alexa-488 (A-11034, diluted to 4 μg/ml, Molecular Probes). The slides were observed with a confocal laser scanning microscope (TCS SP8, Leica).

(4) *In situ* hybridization

Preparing RNA probes

For preparing cRNA probes, I amplified the DNA fragments of zebrafish *six7* and various phototransduction genes by PCR from retinal cDNAs of adult zebrafish with primers listed in table 2. The amplified cDNA fragments were cloned into pGEM15H vector (46) or into pCR4Blunt-TOPO (K2875-20SP, Life Technologies). The resultant plasmids were linearized with appropriate restriction enzymes, and then transcribed into digoxigenin (DIG)-labelled RNA with DIG RNA labelling kit SP6/T7 (1175025, Roche) and/or with T3 RNA polymerase (Roche). To separately visualize distinct subtypes of duplicated green (*rh2-1, rh2-2, rh2-3* and *rh2-4*) and red opsin genes (*lws1* and *lws2*), cRNA probes were designed to recognize each 3' UTR region of duplicated opsin genes according to the previous study (34). The *lws1/2* cRNA probe was designed in the coding region of *lws1* to visualize both *lws1* and *lws2* mRNA and generated in previous study (46). The *rho* cRNA probe was also generated in previous study (46). The *rh2-1/2* cRNA probe was designed in the coding region of *rh2-2* to visualize both *rh2-1* and *rh2-2.*

以下、5 年以内に雑誌等で刊行予定のため、非公開。

Table 2.

PCR primers used to amplify the target gene fragments for preparing cRNA probes.

Target gene	Forward (5' to 3')	Reverse (5' to 3')
sws1	CCTCAGAGGTTTCCAGCAAG	TTGGACAGGAGCAGACAGTG
sws2	GGGAGGTGACAAAGATGGTG	ATGTTCAGCAAGCCAAGACC
rh2-1	ATCTGCCTATTCAGTGCTCC	TGGAATGCATGCTTTTATTTAA
rh2-2	AACTAATTGCCAACTATGCTTTC	TTTGAATGCATGTATTTATTATTCTAC
rh2-3	ACTTTTTGAACTTCTTTGTGG	CACTTTTAATGCCAGTATTTATTC
rh2-4	TCTTTTGAACTTCTTTACAGGTTATG	TTTTTAATGCCGGTATTTATTTC
rh2-1/2	CGTTCCTGTTACAACCATC	ACGCTGGAGACACAGAGGAC
lws1	AGTCAGACATGGGGAAAAAG	TACATGGGCAGGCATCTAC
lws2	TGAACAAGAGGGAAGAACTG	GTACAACATATCATTTTGCTGC
six7	TTGCTTATCTTTCCTTTAAT	ACATCTAGCCTCTGTTTCCAAC

以下、5 年以内に雑誌等で刊行予定のため、非公開。

Whole-mount *in situ* hybridization

Whole-mount *in situ* hybridization was performed as described previously (44) with some modifications. Larval zebrafish were fixed in 4% paraformaldehyde (PFA) in D-PBS overnight at 4°C, dehydrated through a methanol series and stored in 100% methanol at -20°C. At least one day later, the samples were rehydrated and pre-treated with 10 µg/ml proteinase K in PBST (0.1% Tween 20 in D-PBS) for 12 min [for the larvae at 1.5 days post fertilization (dpf)] or for 20 min (for the 2-dpf and 2.5-dpf larvae). The pre-treated larvae were re-fixed in 4% PFA in PBST for 30 min and washed four times with PBST. The treated samples soaked in HYB+ [50% formamide, 5x standard saline citrate (SSC), 0.1 % Tween 20, 1 mg/ml Yeast tRNA, 50 µg/ml heparin], then hybridized with ~2 µg/mL DIG-labelled RNA probes in HYB+ at 65 °C for at least 16 hr. The hybridized samples were washed sequentially with 75%, 50%, 25% and 0% HYB (HYB+ without the yeast tRNA and the heparin) in 2x SSC at 65 °C for 10 min, and further washed twice with 0.2x SSC at 65 °C for 25 min. After several washes with PBST, the specimens were incubated in a blocking solution (1% bovine serum albumin,

2% goat normal serum, 0.1% Tween 20 in PBS) for 2 hr at room temperature, and then treated with Anti-Digoxigenin-AP (diluted 1:2000, Roche) in 0.5x blocking solution in PBST overnight at 4°C. The treated samples were washed six times with PBST, and soaked in alkaline tris buffer (100 mM Tris-HCl, 50 mM $MgCl_2$, 100 mM NaCl, 0.1 % Tween 20, pH 9.5). Then, hybridization signals were visualized by incubating in NBT/BCIP solution (225 µg/ml NBT and 175 µg/ml BCIP in alkaline tris buffer). The staining reaction was terminated by fixation in 4% PFA in PBST. After the termination, the specimens were washed sequentially with 30% and 75% methanol in PBST for 5 min each and washed twice in 100% methanol. Then, the specimens were immersed sequentially in 30%, 50% and 70% glycerol in PBST for 5 min each, and subjected to examination with a stereoscopic microscope (MZ-FL3, Leica).

In situ hybridization using larval and adult ocular sections

In situ hybridization using larval and adult ocular sections was carried out essentially as described previously (46, 47). The 10-µm frozen ocular sections were prepared in a similar manner as described above for immunohistochemistry. These sections were fixed in 4% PFA in PB (77.4 mM Na_2HPO_4, 22.6 mM NaH_2PO_4, pH 7.4) for 15 min, rinsed with PB and treated with 5 µg/mL Proteinase K in TE (10 mM Tris-HCl, 1 mM EDTA, pH 8.0) at 37°C for 15 min. The treated sections were refixed in 4% PFA in PB for 10 min, washed with PB and incubated in 0.2 N HCl for 10 min. After wash with PB, the specimens were soaked in TEA (100 mM triethanolamine, pH 8.0) for 1 min and incubated in TEA with 0.25% acetic anhydride for 10 min followed by a 1 min-rinse in PB. The pre-hybridized samples were hybridized with the DIG-labelled RNA probes in a hybridization buffer (50% formamide, 10% dextran sulfate, 10 mM Tris-HCl, 0.2 mg/mL yeast tRNA, 1x Denhardt's solution, 600 mM NaCl, 0.25% SDS, 1 mM EDTA, pH 7.5) at 65°C for at least 16 hr. The concentration of the RNA probes

was as follows: ~1 μg/mL for the opsin probes and ~2 μg/mL for the *six7* probe. Post-hybridization washes were also performed at 65°C. The hybridized slides were washed sequentially with 50% formamide in 2x SSC for 30 min, with 2x SSC for 20 min and twice with 0.2x SSC for 20 min. The washed samples were soaked in buffer 1 (100 mM Tris-HCl, 150 mM NaCl, pH 7.5) for 5 min, incubated in a blocking solution [1.5% Blocking Reagent (Roche) in buffer 1] for 1 hr at room temperature, and then with Anti-Digoxigenin-AP (diluted 1:2000) in the blocking solution overnight at 4°C. The treated samples were washed twice with buffer 1 for 15 min, and soaked in buffer 3 (100 mM Tris-HCl, 50 mM $MgCl_2$, 100 mM NaCl, pH 9.5) for 15 min. Then, hybridization signals were visualized by incubating in NBT/BCIP solution (450 μg/ml NBT and 175 μg/ml BCIP in buffer 3). The staining reaction was terminated by incubation in a stopping buffer (10 mM Tris-HCl, 1mM EDTA, pH7.5) for 5 min and/or by fixation in 4% PFA in PB for 10 min. The treated slides are washed with PBS, then coverslipped in 50% glycerol in PBS, and subjected to examination with a microscope, Axioplan2 (Carl Zeiss) or BZ-9000 Generation II (Keyence).

(5) RNA extraction and RT-qPCR

All the zebrafish were sampled during the light phase. The eye of adult zebrafish was soaked in RNA*later* (R0901, Sigma) and stored at 4°C. On the other hand, the larvae were dissected into anterior and posterior segments. The posterior ones were used for the genotyping, while the anterior segments were soaked in RNA*later* and stored at 4°C. After genotyping, the larval eyes were isolated with dressmaker pin. Total RNA was extracted and purified using the RNeasy Micro Kit (Qiagen) or the RNeasy Mini Kit (Qiagen) from the eyes of adult or larval zebrafish. After measurement of the concentration of the total RNA, the equal amounts of RNA among samples were reverse-transcribed into cDNA using the oligo $(dT)_{15}$ primer with GoScript™ Reverse Transcriptase (A5003, Promega). The resultant cDNA was subjected to quantitative

PCR by using GoTaq qPCR Master Mix (A6001, Promega) and the StepOnePlus™ Real-time PCR system (Applied Biosystems). The amounts of cDNA were quantified following the manufacturer's protocol. The primers used for quantitative PCR were listed in table 3. For green and red opsin genes, the primers were designed to recognize both of *rh2-1* and *rh2-2* green opsin genes and both of *lws1* and *lws2* red opsin genes, which refer to as *rh2-1/2* and *lws1/2,* respectively. In all the figures, the mRNA levels were normalized to beta-actin 2 (*actb2*) mRNA levels.

以下、5 年以内に雑誌等で刊行予定のため、非公開。

Table 3.

Primers used for RT-qPCR.

Target gene	Forward (5' to 3')	Reverse (5' to 3')
sws1	CGAGAGATATGTGGTCATCTG	TGTATCTGCTCCATCCAAAG
sws2	GGAGGAATGGTGAGTTTGTG	GGTCTTGAAGGTAAAGTTCC
rh2-1	GTAATGGAGGGATTCTTCGC	TGGTCCGCAAGAGGTTTG
rh2-2	GCGTGGGTAGATTAGTTGTG	GGCTTATGCTCAGATTTAGTGG
rh2-3	AGGAAACAAAAACAGCATTG	ATACAGTATAAATGACAGCCTTC
rh2-4	CTGAGAAATCTGGGCATCTG	TGGCGTGTAGAAAATATAAC
rh2-1/2	GGAGGTCAGGTTGCTCTTTG	GACCAGCCAAAAAGTGGG
lws1	TACCTGGCCATCCATGCTG	GGCGAAGAACGTGTAAGGAC
lws2	ATGCCTGCCTACTTTGCC	CCAGTTCTTCCCTCTTGTTC
lws1/2	CATTCTCTGCTACATTGCTG	CATTCTGGACACTTCCTTC
rho	TCCGAGACCACACAGCG	CTGCTTGTTCATGCAGATG
gnat1	AGATGCCAGGACCGTCAAAC	CAAGGGAGTAACCATCTTTGTG
gnat2	ATGCCGATAAGGAAGCCAAG	ATAACCACCTTGATGGAGAATC
arr3a	CTGATAAGCCTGTTCTTCTG	GTGGTTTGGTCAACTGTAAC
arr3b	GCAAGGCGTTGTTGTTTCC	ATGTGAGGCTTCCCAAGAGTC
nr2e3	TTCAGAGACCAGGTGATTC	CAGTTGTCCAGAGGTAGAGAC
nrl	CTACAAACGTCTCCAGCACC	AAGGCGAGGTGTTAGGATG
crx	CATAACTGGAGGGGAATCTG	AAAGCACGACACAAGAACTC
otx5	GAAGAAGTGGCTCTCAAGATC	AAACCAGACCTGGACTCTAGAC
tbx2b	CGACTCTGATGCTTCCTCAAG	GTCCATTTCGTGCTCGCTATC
six7	CTGCAGGACCCTTATCCAAAC	CATTCAGGAGAACTTCCAGAC
thrb1/2 (isoform1 + isoform2)	AACTTGGACGATTCAGAGGTG	TGAGCCACCTTGTGCTTACG
thrb2 (isoform 2: ENSDART00000170790.1)	CTCAGTCACTATCACCAACAAG	TGTCTCCACAAACAACACAC
actb2	GGCAATGAGAGGTTCAGGTG	GTGGTACCACCAGACAATAC

以下、5 年以内に雑誌等で刊行予定のため、非公開。

(6) Immunoblotting

For immunoblot analysis, eyes were dissected from adult zebrafish and homogenized with ice-cold buffer A (10 mM HEPES-NaOH, 10 mM KCl, 0.1 mM EDTA, 1 mM dithiothreitol, 1 mM phenylmethylsulfonyl fluoride, 4 μg/ml aprotinin, 4 μg/ml leupeptin, pH 7.8). The homogenate was centrifuged (5 min at 700 × *g*), and the supernatant was collected (cytosolic fraction). The precipitate was washed in buffer A and centrifuged again, and the precipitate (nuclear fraction) was lysed in SDS-PAGE sampling buffer (10 mM Tris-HCl, 6% glycerol, 2% SDS, 50 mM dithiothreitol, 2 mM EDTA and 0.02% Coomassie Brilliant Blue R-250, pH 6.8). Proteins in the tissue homogenates were separated on an SDS-PAGE and were transferred to a polyvinylidene difluoride membrane (Immobilon-P transfer membrane; Millipore). The blotted membrane was pre-incubated with 1% (w/v) skim milk (BD Diagnostic Systems) in TBS (50 mM Tris-HCl, 200 mM NaCl, 1 mM $MgCl_2$, pH7.4) for 1 h at 37°C for blocking. The membrane was then incubated with one of the following primary antibodies in the blocking solution overnight at 4°C: 5 年以内に雑誌等で刊行予定のため、非公開。The primary antibodies were detected by horseradish peroxidase-conjugated anti-mouse IgG (diluted to 0.2 μg/ml, 074-1816, Kirkegaard & Perry Laboratories) or anti-rabbit IgG (diluted to 0.2 μg/ml, 074-1516, Kirkegaard & Perry Laboratories) in combination with an enhanced chemiluminescence detection system using Western Lightning Chemiluminescence Reagent (PerkinElmer Life Sciences) or ImmunoStar (Wako Pure Chemical Industries). Images were acquired with ImageQuant LAS 4000 mini (GE healthcare).

(7) Sequence alignment and phylogenetic analysis

I selected representative clades of vertebrate and invertebrate for phylogenetic analysis, and obtained amino acid sequences of the *sine oculis* homeobox (Six) protein

family members and the green cone opsins (Rh2) from the Ensembl genome browser (http://www.ensembl.org). For elephant shark, the amino acid sequences of SIX protein family members were retrieved from the database of Elephant Shark Genome Project (http://esharkgenome.imcb.a-star.edu.sg/). Accession numbers used for alignment are listed in table 4 and table 5. *SIX7* candidates were searched in the NCBI genome database by tBLASTn searches using the sequence of green anole SIX7-like protein. I identified two SIX7-like protein in green sea turtle and Indian python. For construction of phylogenetic tree of the Six protein family with and without reptile *SIX7*-like sequence, I used SIX domain and homeodomain amino acid sequences (143 and 173 amino acids), respectively. For construction of phylogenetic tree of teleost green cone opsins, I used full-length amino acid sequences without N- and C- terminal regions (about 310 amino acids) were used. The phylogenetic tree was built by the neighbor-joining method with 1,000 bootstrap replicates using CLC Main Workbench 6 software. Nematode CEH-34 was used as an outgroup for Six family members, while spotted gar Rh2 was used as an outgroup for teleost green cone opsins.

(8) Calculation of the larval eye area

For generating *six7/six3b* double knock-out zebrafish and WT siblings, the *six3b*$^{ja53/+}$ fish were crossed with *six7*$^{ja52/+}$ fish to generate *six7*$^{ja52/+}$;*six3b*$^{ja53/+}$ fish. The resultant fish were crossed with each other to generate *six7* and/or *six3b* knock-out zebrafish. Then, I crossed of *six7*$^{ja52/+}$;*six3b*$^{ja53/+}$ double heterozygous fish and obtained the larvae with one of nine genotypes.

The images were taken with a stereoscopic microscope (MZ-FL3, Leica) and subjected to measurement of the eye area with ImageJ software.

Table 4.

Accession numbers used for alignment of the members of Six family.

Vertebrate species	Gene	Accession number
human (*Homo sapiens*)	*SIX1*	ENSP00000247182
	SIX2	ENSP00000304502
	SIX3	ENSP00000260653
	SIX4	ENSP00000216513
	SIX5	ENSP00000316842
	SIX6	ENSP00000328596
Chinese soft-shell turtle (*Pelodiscus sinensis*)	*SIX2*	ENSPSIP00000009496
	SIX3	ENSPSIP00000009008
	SIX6	ENSPSIP00000016433
	SIX7	ENSPSIP00000016631
anole lizard (*Anolis carolinensis*)	*SIX7*	ENSACAP00000021004
green sea turtle (*Chelonia mydas*)	*SIX7*	XP_007057958.1
Indian python (*Python molurus*)	*SIX7*	XP_007426202.1
coelacanth (*Latimeria chalumnae*)	*SIX1*	ENSLACP00000021104
	SIX2	ENSLACP00000015908
	SIX3	ENSLACP00000017069
	SIX4	ENSLACP00000021088
	SIX5	ENSLACP00000014916
	SIX6	ENSLACP00000021143
zebrafish (*Danio rerio*)	*six1a*	ENSDARP00000057431
	six1b	ENSDARP00000028379
	six2a	ENSDARP00000075251
	six2b	ENSDARP00000071623
	six3a	ENSDARP00000075254
	six3b	ENSDARP00000071625
	six4a	ENSDARP00000126511
	six4b	ENSDARP00000104361
	six5	ENSDARP00000123087
	six6a	ENSDARP00000098430
	six6b	ENSDARP00000110487
	six7	ENSDARP00000093395
medaka (*Oryzias latipes*)	*six1b*	ENSORLP00000019739
	six2a	ENSORLP00000005562
	six3a	ENSORLP00000005568
	six3b	ENSORLP00000012924
	six4b	ENSORLP00000019732
	six5	ENSORLP00000008488
	six6	ENSORLP00000019744
	six7	ENSORLP00000010004
spotted gar (*Lepisosteus oculatus*)	*six1*	ENSLOCP00000012336
	six2	ENSLOCP00000020213
	six3	ENSLOCP00000020214

	six4	ENSLOCP00000012349
	six5	ENSLOCP00000018274
	six6	ENSLOCP00000012326
	six7	ENSLOCP00000001894
elephantshark (*Callorhinchus milii*)	*SIX1*	SINCAMP00000004524
	SIX2	SINCAMP00000018264
	SIX3	SINCAMP00000012754
	SIX4	SINCAMP00000004532
	SIX6	SINCAMP00000004521
lamprey (*Petromyzon marinus*)	*SIX3*	ENSPMAP00000002840
nematode (*Caenorhabditis elegans*)	*ceh-34*	C10G8.6

Table 5.

Ensembl accession numbers used for alignment of the members of the green cone opsins in ray-finned fish.

Vertebrate species	Gene	Ensembl accession number
zebrafish (*Danio rerio*)	*rh2-1*	ENSDARP00000001158
	rh2-2	ENSDARP00000011837
	rh2-3	ENSDARP00000001943
	rh2-4	ENSDARP00000000979
cod (*Gadus morhua*)	*rh2-1*	ENSGMOP00000018628
	rh2-2	ENSGMOP00000018611
fugu (*Takifugu rubripes*)	*rh2-2*	ENSTRUP00000005472
stickleback (*Gasterosteus aculeatus*)	*rh2-1*	ENSGACP00000001857
	rh2-2	ENSGACP00000001853
tilapia (*Oreochromis niloticus*)	*rh2-Aa*	ENSONIP00000005293
	rh2-Ab	ENSONIP00000005291
	rh2-B	ENSONIP00000005294
platyfish (*Xiphophorus maculatus*)	*rh2-1*	ENSXMAP00000015304
	rh2-2	ENSXMAP00000015295
medaka (*Oryzias latipes*)	*rh2-A*	ENSORLP00000024993
	rh2-B	ENSORLP00000024987
	rh2-C	ENSORLP00000024943
spotted gar (*Lepisosteus oculatus*)	*rh2*	ENSLOCP00000015272

3-1. Results

(1) Cone-specific expression of *six7*

I compared gene expression profiles between rod and cone cells purified from the adult zebrafish retina in our microarray analysis (Shiraki *et al.* to be published). Among ~500 genes that were highly expressed in cones (>10 times), I focused on *sine oculis homeobox homolog 7* (*six7)*, whose signal intensity was the highest among the cone-enriched transcription factors in our microarray analysis. Six7 belongs to Six family, and Six7 is found in ray-finned fish, while a full-length cording sequence of *six7* was not found in any other vertebrate species (figure 3). The phylogenetic tree of Six family showed that Six7 is a member of Six3/Six6/Six7 group, and Six7 subfamily was separated before the divergence between Six3 and Six6 subfamilies. Considering that both of Six3 and Six6 subfamilies are widely conserved in vertebrate species (figure 3), the early separation of Six7 from Six3/Six6 group implies the presence of *six7* in the ancient vertebrates.

I investigated the expression pattern of *six7* in zebrafish. RT-qPCR analysis with purified cones and rods revealed that *six7* was far more highly expressed in cones than in isolated rods (>10 times; figure 4a). Among the adult tissues, the expression of *six7* was mainly detected in the retina (figure 4b). Then, I checked the expression pattern of *six7* in the adult retina by *in situ* hybridization with cryosections, and found that *six7* was expressed specifically in the photoreceptor layer at the adult stage (figure 4d). In particular, the *six7*-positive signal was mainly detected in the cone layer, where the red and green cones are located (figure 4e). The cone-specific expression of *six7* suggest that *six7* have a key role for the development of cone photoreceptors.

To examine a role of *six7* for the development of cone photoreceptors, I checked gene expression profiles of *six7* during the retinal development in addition to the adult

stage. The expression of *six7* was detected in the anterior region but not in the posterior region of the larvae and in the eyes at four days post fertilization (4 dpf) (figure 4c). Then, I performed whole-mount *in situ* hybridization and confirmed eye-specific expression of *six7* (figure 4f). The *six7* expression in the eye was observed in the larval zebrafish at 1.5 dpf, about when zebrafish retinal development just begins. The spatio-temporally regulated expression pattern of *six7* suggests that *six7* is expressed in the retinal progenitor cells. I also checked the expression of *six7* by *in situ* hybridization using cryosections of 3.5-dpf zebrafish larvae, and found that *six7*-positive cells were only in the photoreceptor cell layer (figure 4g). At this developmental stage, cones are distributed uniformly across the whole retina (48), while rods are tightly clustered in the ventral retina (48). The distribution pattern of the *six7*-positive cells was similar to that of the cone-specific phototransduction component genes (48). Although the expression pattern does not deny the *six7* expression in rods at the larval stages, these results imply the predominant expression of *six7* in cones at 3.5 dpf and suggest a role of *six7* in the cone development.

(2) Decrease of green and blue cones in *six7* knock-out zebrafish at the larval stage

To investigate a role of *six7* in the development of photoreceptors, three lines of *six7* knock-out zebrafish were generated with TAL effector nucleases (TALENs): the *six7*^{ja51}, *six7*^{ja52} and *six7*^{ja54} (figure 5a and 5b). The nucleotide deletion is in the *six7* coding region of the mutant zebrafish: 8-bp loss in the *six7*^{ja51} zebrafish caused a frame shift of the amino acid sequence of Six7, and introduced an immature stop codon. 13-bp loss in the *six7*^{ja52} zebrafish also caused the loss of Six7 protein, and 6-bp loss in the *six7*^{ja54} zebrafish change codon 18 (asparagine) to stop, thus also caused the *six7* deficiency.

I performed RT-qPCR analysis with the *six7*$^{ja51/ja51}$ knock-out zebrafish larvae, and checked the effect of the loss of *six7* on the expression levels of phototransduction component genes. Notably, the expression levels of the green opsins (*rh2-1* and *rh2-2*) and blue opsin (*sws2*) were reduced in 3.5-dpf *six7*$^{ja51/ja51}$ larvae (figure 5c). Teleost often has multiple copies of green opsin genes by gene duplication, and the developmental stage-dependent expression is observed in these green opsin genes. Similar to other teleosts, zebrafish has many copies of green opsin genes: *rh2-1, rh2-2, rh2-3* and *rh2-4*. The expression of *rh2-3* and *rh2-4* are hardly detected during larval stage in both the wild-type larvae (34) and the *six7*$^{ja51/ja51}$ knock-out larvae (data not shown). Thus, I focused on *rh2-1* and *rh2-2* for examination of the expression level of the green opsin genes.

In situ hybridization analysis (figure 5f) showed that the green opsin (*rh2-1* and/or *rh2-2*) expressing cells were hardly detected in the *six7*$^{ja51/ja51}$ knock-out larvae. On the other hand, the expression of blue opsin gene (*sws2*) was reduced in the *six7*$^{ja51/ja51}$ larvae to the same extent (approximately by half) as in RT-qPCR analysis, suggesting the decreases in the numbers of middle wavelength-sensitive cones; *i.e.*, green and blue cones. In addition, *six7*$^{ja51/ja51}$ larvae showed reduced expression levels of cone subtype-specific phototransduction gene: arrestin 3a (*arr3a*) and arrestin 3b (*arr3b*) (figure 5c). The expression of *arr3a* and *arr3b* is detected in the double cones (green and red cones) and the single cones (UV and blue cones), respectively (49). The reduced expression levels of phototransduction component genes further supports the reduction of the number of blue and green cones in *six7*$^{ja51/ja51}$ larvae at 3.5 dpf.

The reduced expression levels of blue and green opsin genes were also observed in another *six7* mutant larvae, *six7*$^{ja52/ja52}$ (figure 5d). The expression profiles of rod and cone opsin genes in the *six7*$^{ja52/ja52}$ knock-out larvae were very similar to those in the *six7*$^{ja51/ja51}$ knock-out larvae, suggesting that the expression levels of opsin genes in the *six7* mutants were altered by the deficiency of *six7* and not by any off-target effect of

TALENs. Furthermore, using *six7*^{ja52} line, I tested whether the loss of *six7* and *six3b* caused the loss of the eyes at the larval stage. The eye loss was previously reported in *six7/six3b*-deficient larvae by blocking the translational start site of *six7* with morpholino oligonucleotides (39). Thus, I generated the *six7*$^{ja52/ja52}$ and *six3b*$^{ja53/ja53}$ double knock-out larvae and found that the double mutant had extremely small eyes (figure 6). These results confirm that the deficiency of *six7* is caused by the ja52 mutation. In the following experiments, I used *six7*$^{ja51/ja51}$ zebrafish, which refer to as *six7* KO.

In contrast to the redundant role of *six3b* and *six7* during the eye development [(39) and figure 6], the loss of *six3b* caused no significant alteration of mRNA levels of the opsin genes (figure 6c). These results suggest that *six7* plays specialized roles in regulating the expression of cone opsin genes.

(3) Increase of rod photoreceptors in *six7* knock-out zebrafish at the larval stage

In contrast to the marked reduction of blue and green cone cells in the *six7* knock-out zebrafish, the expression levels of rod-specific phototransduction component genes, rhodopsin (*rho*) and rod transducin α-subunit (*gnat1*), were increased in *six7* KO larvae as compared to WT (figure 5e). Immunohistochemistry with anti-Gnat1 antibody confirmed the increase of rods in *six7* KO larvae (figure 5g). The upregulated expression levels of rod-specific transcription factors, neural retina leucine zipper (*nrl*) and nuclear receptor subfamily 2, group E, member 3 (*nr2e3*) was also observed in *six7* KO (figure 5e). These two transcription factors are proved to be an essential regulators for the rod development in mice (20, 21). Collectively, these results verified that the loss of *six7* increased rod cells at 3.5 dpf.

(4) Decrease of green cones in *six7* knock-out zebrafish at the adult stage

To examine whether the severely reduced number of green cone photoreceptors caused by the loss of *six7* was observed throughout developmental stages, I analyzed expression profiles of phototransduction component genes in the adult eyes by RT-qPCR and *in situ* hybridization. The *six7* deficiency reduced the expression levels of all the green opsin genes and the number of all the subsets of green cones at the adult stage (figure 7a and 7d), indicating that *six7* is essential for development of green cones.

(5) Distinct phenotypes between the larval and adult stages for blue cones, red cones and rods of *six7* knock-out zebrafish

The loss of the green cones in *six7* knock-out zebrafish was observed at both the larval and adult stages, while the expression levels of rod-specific genes, *rho* and *gnat1*, were not significantly different between wild-type and *six7* knock-out zebrafish at the adult stage (figure 7a). Similarly, RT-qPCR analysis revealed the down-regulated expression of blue opsin gene in *six7* knock-out only at the larval stage (figure 5c and 5d) but not at the adult stage (figure 7a). In contrast to the result of RT-qPCR, *in situ* hybridization analysis with ocular section of adult zebrafish showed reduction of the number of blue cone in the adult *six7* KO central retina, where early differentiated photoreceptors were located (figure 7d). These results suggested that *six7* is essential for the development of blue cones only at the larval stage.

Stage-dependent effect of the loss of *six7* is also observed for the expression of red cone opsin genes. In contrast to the rods and blue cones, the mRNA levels of red cone opsin genes were altered only at the adult stage (figure 7 and figure 8). Two duplicated red opsin genes (*lws1* and *lws2*) are in zebrafish genome, and their expression patterns in the retina are spatio-temporally regulated (34, 50). RT-qPCR analysis showed that the *lws1* expression level was remarkably increased in the adult

eye of *six7* knock-out (figure 7a), while in the larval eye, the *lws1* expression was not affected by the loss of *six7* (figure 5c and 5d). *In situ* hybridization analysis confirmed that spatial distribution pattern of *lws1*-positive red cones in the adult *six7* knock-out retina was also different from that in the adult wild-type retina. In wild-type, the *lws1*-expressing red cones were confined to the peripheral retina, while the *lws2*-expressing red cones were localized in the central retina (figure 7d, figure 8b). In *six7* knock-out, the *lws1*-positive red cones were distributed across the whole retina (figure 7d, figure 8). At 3-mpf adult stage, *in situ* hybridization analysis revealed that the loss of *six7* mostly unaffected the expression of *lws2* in the central retina (figure 7d), which is consistent with the RT-qPCR analysis (figure 7a). However, surprisingly, at the later stage (4 mpf) the expression level of *lws2* was severely reduced in the central retina of *six7* knock-out zebrafish (figure 7d, figure 8). Considering that the *six7* knock-out larvae exhibited the normal development of red cones (figure 5) and that the laminar structure of the retina was not affected by the loss of *six7* throughout the developmental stages (figure 7), I assume that *six7* regulates only the expression levels of the *lws1* and *lws2* red opsin genes in the red cones. To further validate the number of red cone photoreceptor cells, I conducted whole-mount immunohistochemistry with the adult retina and compared the number of the red cones between wild-type and *six7* knock-out zebrafish. The number of the Gnat2-positive cells in the double cone layer was decreased by the loss of *six7*, while the number of red cones was not apparently altered in the 6-mpf adult retina of *six7* knock-out (figure 8c). Collectively, the *six7* deficiency is likely to cause a co-expression of *lws1* and *lws2* in the central retina and then to cause gradual switching of the expression of red opsins from *lws2* to *lws1* without affecting total number of the red cones. These results suggest that *six7* is also essential for the spatio-temporally regulated expression of the duplicated red opsin genes.

3-2. Results

5 年以内に雑誌等で刊行予定のため、非公開。

This chapter will be published within 5 years.

4. Discussion

- **Presence of *SIX7*-like sequences in the genome of reptiles**

So far, many ray-finned fish have *six7* gene but neither birds nor mammals have. The phylogenetic analysis indicated that Six7 subfamily emerged at the early evolutionary stage and that *six7* is lost in some vertebrate species (figure 3). To confirm the presence of *six7* gene in vertebrate species, I searched homologues of *six7* in the Ensembl Genome database, and noticed a gene named *SIX7* in the genome of green anole and Chinese soft-shell turtle. Then, I conducted tBLASTn searches and identified *SIX7*-like sequences in the NCBI genome database of other reptilian species, green sea turtle and Indian python. I aligned amino acid sequences of members of Six protein family including those of reptilian SIX7 (figure 21a), and found that these reptilian Six7 is quite diverged from ray-finned fish Six7: many amino acid differences and gaps were in the sequence alignment (figure 21b). Additional genome information will be required to clarify the presence of *SIX7* genes in vertebrates other than ray-finned fish.

5 年以内に雑誌等で刊行予定のため、非公開。

- **Mutually exclusive expression of duplicated red opsin genes in zebrafish: an attractive model for understanding the color vision in catarrhine primates**

I found that *six7* was involved in the spatio-temporally regulated expression of the duplicated red opsin genes in zebrafish retina (figure 7 and figure 8). Zebrafish red opsin genes are orthologous to human M/LWS opsin genes, which also have emerged from tandem gene duplication. Their spectral sensitivities are diverged from each other and these cone opsins are expressed in a mutually exclusive manner by DNA enhancer (51). The mutually exclusive expression of spectrally distinct red opsin genes

enables red-green color vision in catarrhine primates, while a molecular mechanism underlying the exclusive expression still remains elusive. Similar to human, the DNA region upstream of red opsin genes in zebrafish was identified as an enhancer controlling the expression of two red cone opsin genes (50). In addition, previous studies suggest a conserved regulatory mechanism of the red cone opsin gene between zebrafish and human; the loss of *thrb* reduced the expression level of both of the duplicated red cone opsin genes [our unpublished observation and (31)], and in human, *thrb* is also an attractive candidate for activation of the expression of all the subsets of the duplicated red cone opsin genes (52). Although the distinct origin of the duplicated red opsin genes between teleost and mammals, zebrafish is a suitable animal model for understanding the mechanism of the mutually exclusive expression of duplicated red opsin genes in vertebrates. Recently, the other group have reported that retinoic acid signaling regulates differential expression of the red cone opsin genes in zebrafish (53). A role of the retinoic acid signaling for the development of cone photoreceptors is also suggested by a previous study in mouse (54); loss of retinoid X receptor gamma (*Rxrg*) causes ectopic expression of *SWS1* cone opsin genes. Considering that the loss of *six7* caused the co-expression of two red opsin genes (figure 7 and figure 8), a future analysis on up- or down-regulated genes both by deficiency of *six7* and impaired retinoic acid signaling can lead to understanding the mechanism of the mutually exclusive expression of duplicated red opsin genes.

5. Conclusion

5 年以内に雑誌等で刊行予定のため、非公開。

This chapter will be published within 5 years.

6. References

1. Ebrey T, Koutalos Y (2001) Vertebrate photoreceptors. *Prog Retin Eye Res* 20(1):49–94.
2. Kawamura S, Tachibanaki S (2008) Rod and cone photoreceptors: molecular basis of the difference in their physiology. *Comp Biochem Physiol A Mol Integr Physiol* 150(4):369–77.
3. Lamb TD (2013) Evolution of phototransduction, vertebrate photoreceptors and retina. *Prog Retin Eye Res* 36:52–119.
4. Okano T, Fukada Y, Yoshizawa T (1995) Molecular basis for tetrachromatic color vision. *Comp Biochem Physiol B Biochem Mol Biol* 112:405–414.
5. Goldsmith TH (2013) Evolutionary tinkering with visual photoreception. *Vis Neurosci* 30:21–37.
6. Bowmaker JK (2008) Evolution of vertebrate visual pigments. *Vision Res* 48(20):2022–41.
7. Collin SP, Davies WL, Hart NS, Hunt DM (2009) The evolution of early vertebrate photoreceptors. *Philos Trans R Soc Lond B Biol Sci* 364(1531):2925–40.
8. Yokoyama S (2008) Evolution of dim-light and color vision pigments. *Annu Rev Genomics Hum Genet* 9:259–82.
9. Collin SP, *et al*. (2003) Ancient colour vision: multiple opsin genes in the ancestral vertebrates. *Curr Biol* 13(22):R864-5.
10. Shu D-G, *et al*. (2003) Head and backbone of the Early Cambrian vertebrate Haikouichthys. *Nature* 421(6922):526–529.
11. Lagman D, *et al.* (2013) The vertebrate ancestral repertoire of visual opsins, transducin alpha subunits and oxytocin/vasopressin receptors was established by duplication of their shared genomic region in the two rounds of early vertebrate genome duplications. *BMC Evol Biol* 13(1):238.
12. Novales Flamarique I (2016) Diminished foraging performance of a mutant zebrafish with reduced population of ultraviolet cones. *Proc Biol Sci* 283(1826). doi:10.1098/rspb.2016.0058.
13. Swaroop A, Kim D, Forrest D (2010) Transcriptional regulation of photoreceptor development and homeostasis in the mammalian retina. *Nat Rev Neurosci* 11(8):563–76.
14. Adler R, Raymond PA (2008) Have we achieved a unified model of photoreceptor cell fate specification in vertebrates? *Brain Res* 1192:134–50.
15. Viets K, Eldred KC, Johnston RJ (2016) Mechanisms of Photoreceptor Patterning in Vertebrates and Invertebrates. *Trends Genet* 32(10):638–59.
16. Cepko C (2014) Intrinsically different retinal progenitor cells produce specific types of progeny. *Nat Rev Neurosci* 15(9):615–27.
17. Furukawa T, Morrow EM, Cepko CL (1997) Crx, a novel otx-like homeobox gene, shows photoreceptor-specific expression and regulates photoreceptor differentiation. *Cell* 91(4):531–41.

18. Chen S, *et al.* (1997) Crx, a novel Otx-like paired-homeodomain protein, binds to and transactivates photoreceptor cell-specific genes. *Neuron* 19(5):1017–30.

19. Freund CL, *et al.* (1997) Cone-rod dystrophy due to mutations in a novel photoreceptor-specific homeobox gene (CRX) essential for maintenance of the photoreceptor. *Cell* 91(4):543–53.

20. Chen J, Rattner A, Nathans J (2005) The rod photoreceptor-specific nuclear receptor Nr2e3 represses transcription of multiple cone-specific genes. *J Neurosci* 25(1):118–29.

21. Mears AJ, *et al*. (2001) Nrl is required for rod photoreceptor development. *Nat Genet* 29(4):447–52.

22. Oh ECT, *et al*. (2007) Transformation of cone precursors to functional rod photoreceptors by bZIP transcription factor NRL. *Proc Natl Acad Sci U S A* 104(5):1679–84.

23. Alvarez-Delfin K, *et al*. (2009) Tbx2b is required for ultraviolet photoreceptor cell specification during zebrafish retinal development. *Proc Natl Acad Sci U S A* 106(6):2023–8.

24. Ng L, *et al*. (2001) A thyroid hormone receptor that is required for the development of green cone photoreceptors. *Nat Genet* 27(1):94–8.

25. Hennig AK, Peng G-H, Chen S (2008) Regulation of photoreceptor gene expression by Crx-associated transcription factor network. *Brain Res* 1192:114–33.

26. Onishi A, Peng G-H, Chen S, Blackshaw S (2010) Pias3-dependent SUMOylation controls mammalian cone photoreceptor differentiation. *Nat Neurosci* 13(9):1059–65.

27. Fadool JM, Dowling JE (2008) Zebrafish: a model system for the study of eye genetics. *Prog Retin Eye Res* 27(1):89–110.

28. Stenkamp DL (2007) Neurogenesis in the fish retina. *Int Rev Cytol* 259(6):173–224.

29. Gamse JT, *et al*. (2002) Otx5 regulates genes that show circadian expression in the zebrafish pineal complex. *Nat Genet* 30(1):117–21.

30. Shen Y, Raymond PA (2004) Zebrafish cone-rod (crx) homeobox gene promotes retinogenesis. *Dev Biol* 269(1):237–51.

31. Suzuki SC, *et al*. (2013) Cone photoreceptor types in zebrafish are generated by symmetric terminal divisions of dedicated precursors. *Proc Natl Acad Sci U S A* 110(37):15109–14.

32. Rennison DJ, Owens GL, Taylor JS (2012) Opsin gene duplication and divergence in ray-finned fish. *Mol Phylogenet Evol* 62(3):986–1008.

33. Chinen A, Hamaoka T, Yamada Y, Kawamura S (2003) Gene duplication and spectral diversification of cone visual pigments of zebrafish. *Genetics* 163(2):663–75.

34. Takechi M, Kawamura S (2005) Temporal and spatial changes in the expression pattern of multiple red and green subtype opsin genes during zebrafish development. *J Exp Biol* 208(Pt 7):1337–45.

35. Kawakami K, Sato S, Ozaki H, Ikeda K (2000) Six family genes--structure and function as transcription factors and their roles in development. *Bioessays* 22(7):616–26.

36. Kumar JP (2009) The sine oculis homeobox (SIX) family of transcription factors as regulators of development and disease. *Cell Mol Life Sci* 66(4):565–83.

37. Christensen KL, Patrick AN, McCoy EL, Ford HL (2008) The six family of homeobox genes in development and cancer. *Adv Cancer Res* 101(8):93–126.

38. Seo HC, Drivenes O, Ellingsen S, Fjose A (1998) Transient expression of a novel Six3-related zebrafish gene during gastrulation and eye formation. *Gene* 216(1):39–46.

39. Inbal A, Kim S-H, Shin J, Solnica-Krezel L (2007) Six3 represses nodal activity to establish early brain asymmetry in zebrafish. *Neuron* 55(3):407–15.

40. Dahlem TJ, *et al*. (2012) Simple methods for generating and detecting locus-specific mutations induced with TALENs in the zebrafish genome. *PLoS Genet* 8(8):e1002861.

41. Ogawa Y, Shiraki T, Kojima D, Fukada Y (2015) Homeobox transcription factor Six7 governs expression of green opsin genes in zebrafish. *Proc Biol Sci* 282(1812):20150659.

42. Szczepek M, *et al*. (2007) Structure-based redesign of the dimerization interface reduces the toxicity of zinc-finger nucleases. *Nat Biotechnol* 25(7):786–93.

43. Menger GJ, Koke JR, Cahill GM (2005) Diurnal and circadian retinomotor movements in zebrafish. *Vis Neurosci* 22(2):203–209.

44. Kojima D, Torii M, Fukada Y, Dowling JE (2008) Differential expression of duplicated VAL-opsin genes in the developing zebrafish. *J Neurochem* 104(5):1364–71.

45. Yin J, *et al*. (2012) The 1D4 antibody labels outer segments of long double cone but not rod photoreceptors in zebrafish. *Investig Ophthalmol Vis Sci* 53(8):4943–4951.

46. Mano H, Kojima D, Fukada Y (1999) Exo-rhodopsin: a novel rhodopsin expressed in the zebrafish pineal gland. *Brain Res Mol Brain Res* 73(1–2):110–8.

47. Barthel LK, Raymond PA (2000) In situ hybridization studies of retinal neurons. *Methods Enzymol* 316(1997):579–90.

48. Raymond PA, Barthel LK, Curran GA (1995) Developmental patterning of rod and cone photoreceptors in embryonic zebrafish. *J Comp Neurol* 359(4):537–50.

49. Renninger SL, Gesemann M, Neuhauss SC (2011) Cone arrestin confers cone vision of high temporal resolution in zebrafish larvae. *Eur J Neurosci* 33(4):658–67.

50. Tsujimura T, Hosoya T, Kawamura S (2010) A single enhancer regulating the differential expression of duplicated red-sensitive opsin genes in zebrafish. *PLoS Genet* 6(12):e1001245.

51. Smallwood PM, Wang Y, Nathans J (2002) Role of a locus control region in the mutually exclusive expression of human red and green cone pigment genes. *Proc Natl Acad Sci U S A* 99(2):1008–11.

52. Weiss AH, Kelly JP, Bisset D, Deeb SS (2012) Reduced L- and M- and increased S-cone functions in an infant with thyroid hormone resistance due to mutations in the THRβ2 gene. *Ophthalmic Genet* 33(4):187–95.

53. Mitchell DM, *et al*. (2015) Retinoic Acid Signaling Regulates Differential Expression of the Tandemly-Duplicated Long Wavelength-Sensitive Cone Opsin Genes in Zebrafish. *PLOS Genet* 11(8):e1005483.

54. Roberts MR, Hendrickson A, McGuire CR, Reh TA (2005) Retinoid X receptor (gamma) is necessary to establish the S-opsin gradient in cone photoreceptors of the developing mouse retina. *Invest Ophthalmol Vis Sci* 46(8):2897–904.

55. Asaoka Y, Mano H, Kojima D, Fukada Y (2002) Pineal expression-promoting element (PIPE), a cis-acting element, directs pineal-specific gene expression in zebrafish. *Proc Natl Acad Sci U S A* 99(24):15456–61.

56. Noyes MB, *et al.* (2008) Analysis of homeodomain specificities allows the family-wide prediction of preferred recognition sites. *Cell* 133(7):1277–89.

7. Figures

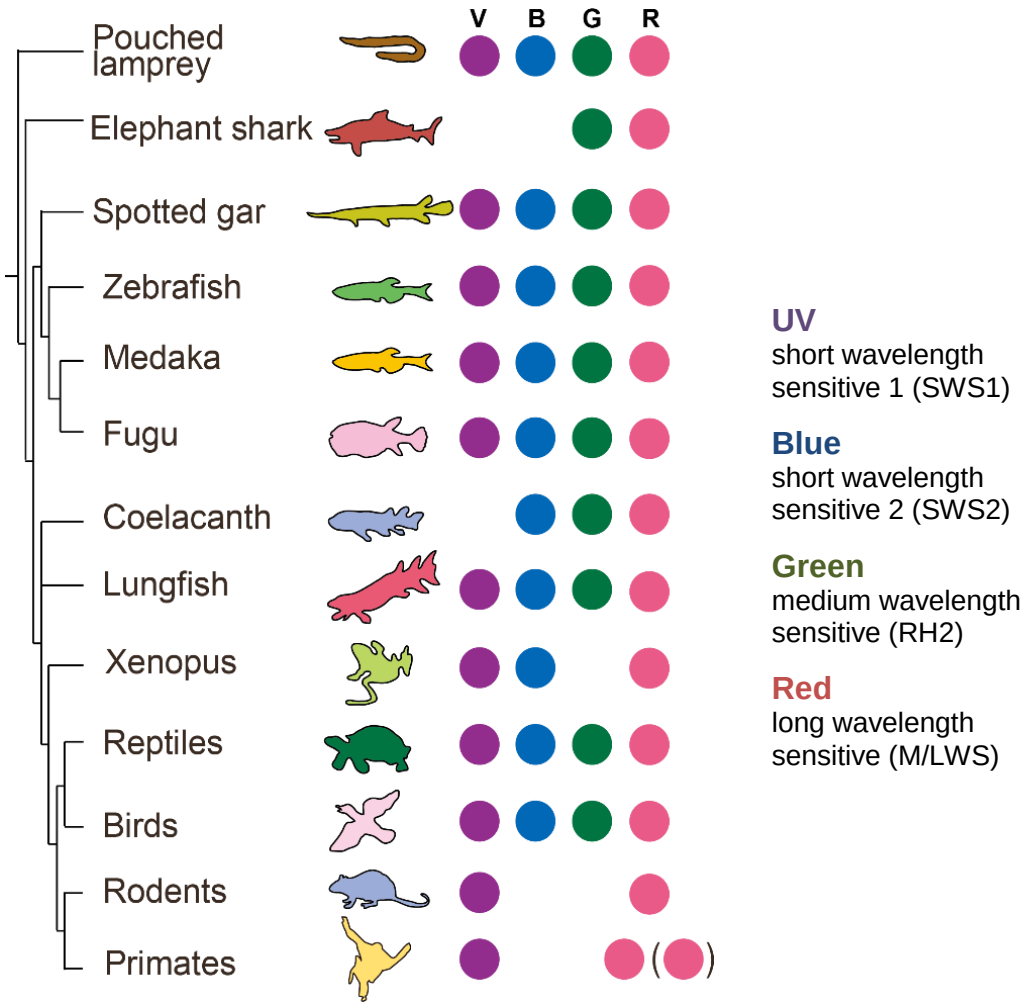

Figure 1. Cone visual opsin genes in vertebrates

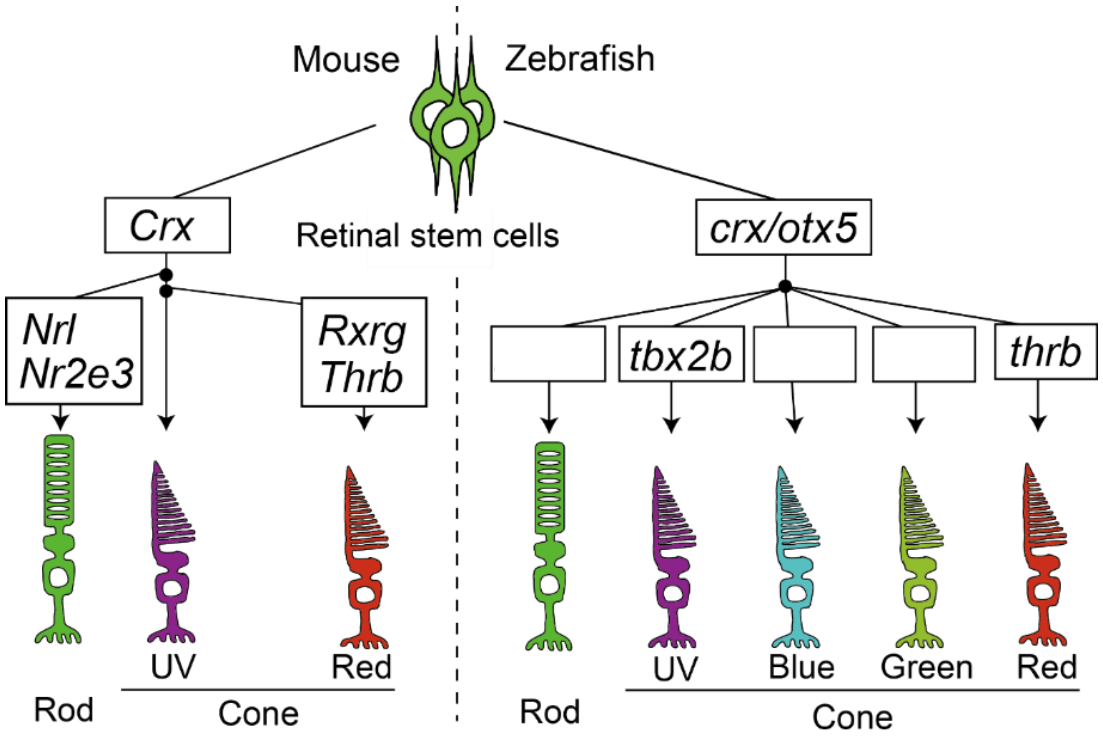

Figure 2. Transcriptional regulation of the gene expression of photoreceptors in mouse and zebrafish

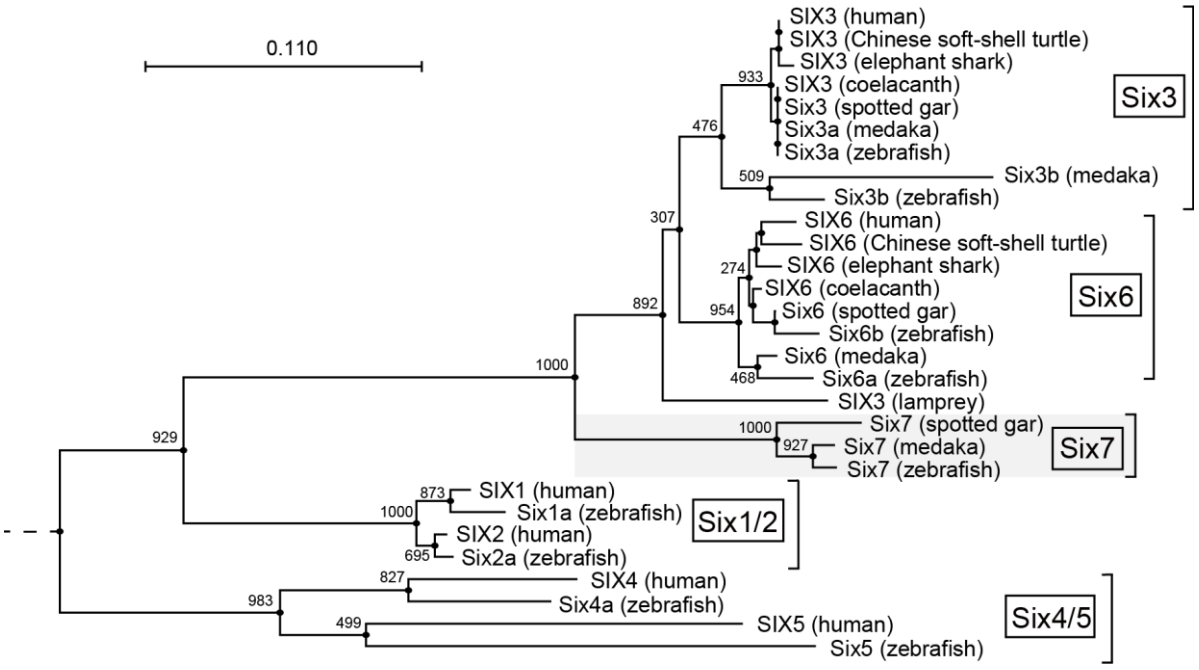

Figure 3. Phylogenetic tree of the members in Six family. A Neighbor-Joining (NJ) tree was constructed with 1,000 bootstrapping replications. Amino acid sequences of SIX domain and homeodomain (173 amino acids) was used for the construction of the NJ tree. Numerical values are indicated at branch nodes. Nematode CEH-34 was used as an outgroup. Scale bar indicates 0.11 substitutions per site. I constructed another phylogenetic tree, which includes additional sequences of Six1/2 and Six4/5 groups and reptile *SIX7*-like sequence. The tree is presented in figure 21.

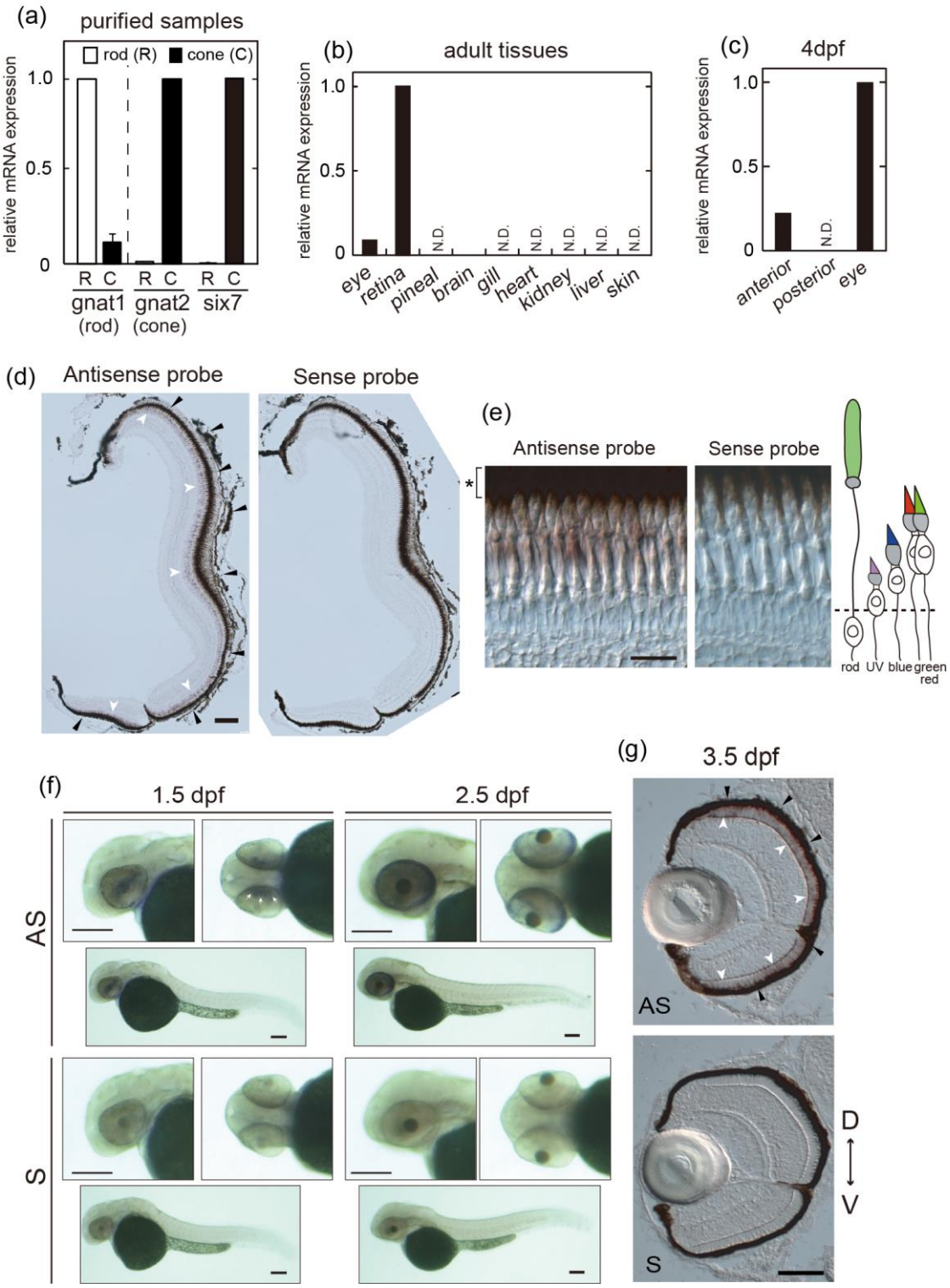
(a)
purified samples
rod (R)
cone (C)
relative mRNA expression
1.0
0.5
0
R C R C R C
gnat1 (rod)
gnat2 (cone)
six7
(b)
adult tissues
relative mRNA expression
1.0
0.5
0
N.D.
eye
retina
pineal
brain
gill
heart
kidney
liver
skin
(c)
4dpf
relative mRNA expression
1.0
0.5
0
N.D.
anterior
posterior
eye
(d)
Antisense probe
Sense probe
(e)
Antisense probe
Sense probe
*
rod
UV
blue
green
red
(f)
1.5 dpf
2.5 dpf
AS
S
(g)
3.5 dpf
AS
S
D
V

Figure 4. Expression patterns of *six7* at the larval and adult stages. (a-c) Relative expression levels of *six7* were measured by RT-qPCR. I quantified the mRNA levels of *six7* in the following samples: (a) isolated rods and cones from *Tg*(*rho:egfp*)*ja2Tg* (55) and *Tg*(*gnat2:egfp*)*ja23Tg* (41) zebrafish, respectively, at the adult stage (n = 2); (b) adult tissues; (c) larval anterior segments, posterior segments and eyes at four days post fertilization (4 dpf). N.D., not detected. (d) The expression pattern of *six7* in the retina of adult zebrafish at seven months post fertilization (7 mpf) by *in situ* hybridization. Cryosections of the adult zebrafish retina were prepared for the experiment. The *six7*-positive cells are localized in the photoreceptor layer (white arrowheads). The retinal pigmented epithelium (RPE, black arrowheads) is adjacent to the photoreceptor layer. Scale bar, 100 µm. (e) Magnified images of (d). The nuclei of the photoreceptor cells are located in distinct layers of the retina among five subtypes of photoreceptor cells (as is shown in the schematic drawing). RPE is showed by the asterisk. Scale bar, 20 µm. (f) The expression pattern of *six7* in the larval zebrafish by whole-mount *in situ* hybridization. I observed the *six7* expression at both 1.5 dpf (arrowheads) and 2.5 dpf. Scale bars, 100 µm. (g) The expression pattern of *six7* in the retina of the larval zebrafish by *in situ* hybridization using ocular sections of the 3.5 dpf-larvae. D, dorsal side. V, ventral side. Scale bar, 50 µm. AS, antisense probe. S, sense probe.

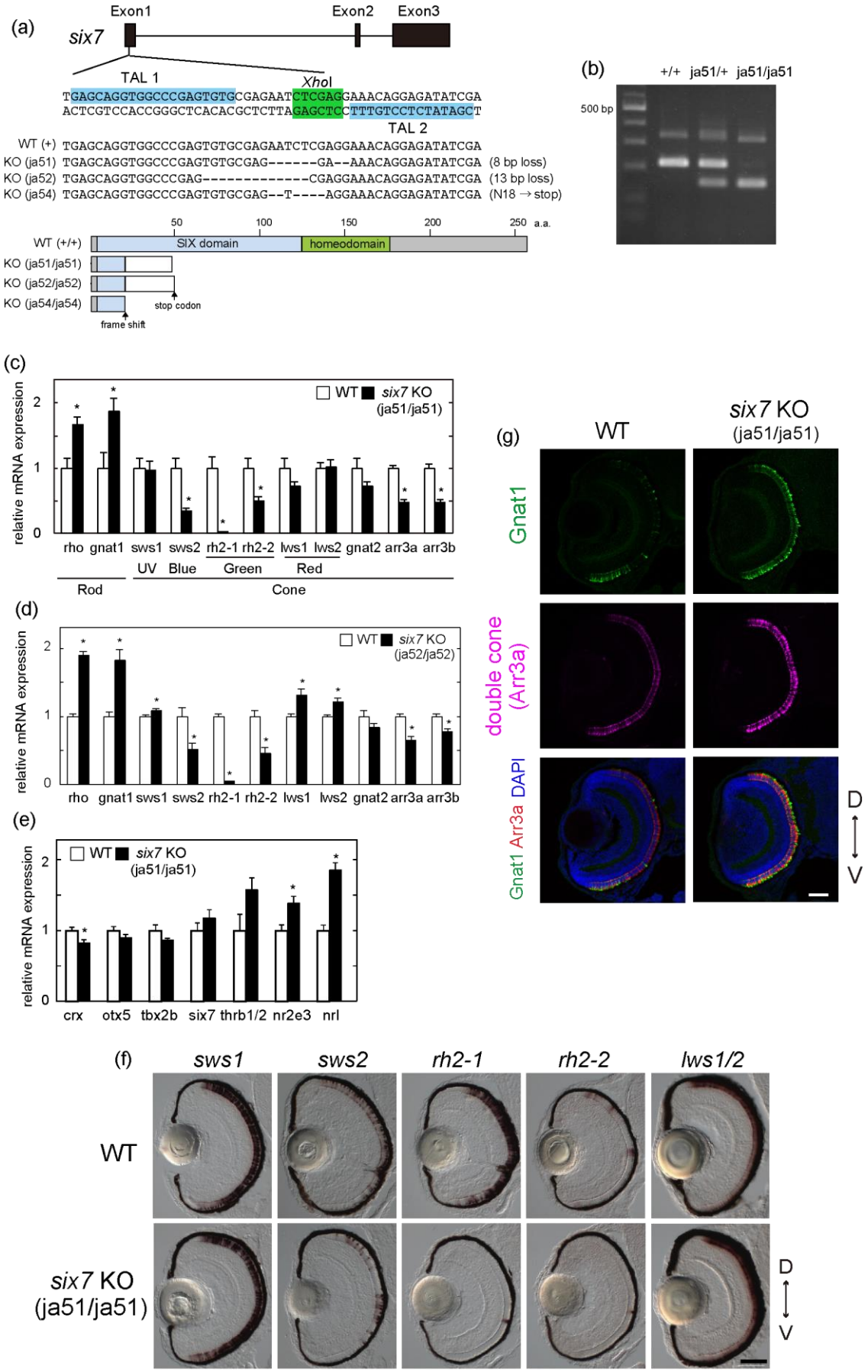
(a)
Exon1
Exon2
Exon3
six7
TAL 1
XhoI
TAL 2
WT (+) TGAGCAGGTGGCCCGAGTGTGCGAGAATCTCGAGGAAACAGGAGATATCGA
KO (ja51) TGAGCAGGTGGCCCGAGTGTGCGAG------GA--AAACAGGAGATATCGA (8 bp loss)
KO (ja52) TGAGCAGGTGGCCCGAG----------CGAGGAAACAGGAGATATCGA (13 bp loss)
KO (ja54) TGAGCAGGTGGCCCGAGTGTGCGAG--T----AGGAAACAGGAGATATCGA (N18 → stop)
50
100
150
200
250 a.a.
WT (+/+)
SIX domain
homeodomain
KO (ja51/ja51)
KO (ja52/ja52)
KO (ja54/ja54)
stop codon
frame shift
(b)
+/+ ja51/+ ja51/ja51
500 bp
(c)
relative mRNA expression
WT six7 KO (ja51/ja51)
rho gnat1 sws1 sws2 rh2-1 rh2-2 lws1 lws2 gnat2 arr3a arr3b
UV Blue Green Red
Rod
Cone
(d)
relative mRNA expression
WT six7 KO (ja52/ja52)
rho gnat1 sws1 sws2 rh2-1 rh2-2 lws1 lws2 gnat2 arr3a arr3b
(e)
relative mRNA expression
WT six7 KO (ja51/ja51)
crx otx5 tbx2b six7 thrb1/2 nr2e3 nrl
(f)
sws1
sws2
rh2-1
rh2-2
lws1/2
WT
six7 KO (ja51/ja51)
D
V
(g)
WT
six7 KO (ja51/ja51)
Gnat1
double cone (Arr3a)
Gnat1 Arr3a DAPI
D
V

Figure 5. Analysis of the wild-type zebrafish (WT) and the *six7* knock-out zebrafish (KO) at the larval stage. (a) *Top*, exon-intron structure and partial nucleotide sequences of zebrafish *six7*. The binding sites of the left and right TALENs are highlighted in *blue*. The recognition site of the endonuclease *Xho*I is highlighted in *green*. *Middle*, the nucleotide sequences of the *six7* KO (ja51, ja52 and ja54 mutant) fish are compared with the WT sequence. Deletions are indicated by dashes. *Bottom*, schematic representations of Six7 and its mutant protein. (b) Genotyping of the *six7* knock-out zebrafish. See Materials and Methods. (c-e) Expression profiles of the phototransduction component genes (c, d) and the transcription factors contributing to the photoreceptor development in mouse and/or zebrafish (e). (c, e) The larval eyes of the WT fish and the *six7* knock-out fish (ja51) at 3.5 dpf. (d) The larval eyes of the WT fish and the other *six7* knock-out fish (ja52) at 4.5 dpf. The mRNA levels were quantified by RT-qPCR. The data are represented by mean + SEM (n = 5). Statistical significance between WT and *six7* KO data is shown as the asterisks (*p<0.05 by Student's t-test). (f) Expression profiles of the cone opsin genes by *in situ* hybridization with the 3.5-dpf larval ocular sections of the WT and *six7*$^{ja51/ja51}$ knock-out fish. The red opsin probe was designed to recognize both of the *lws1* and *lws2* red opsin genes, which refer to as *lws1/2* in this study. D, dorsal side. V, ventral side. Scale bar, 50 μm. (g) Immunofluorescent images of the larval ocular sections of the WT and *six7*$^{ja51/ja51}$ KO zebrafish at 3.5 dpf. The ocular sections were immunostained with the anti-Gnat1 antibody for rods (*green*) and with the zpr1 antibody for double cones (red and green cones) (*magenta*). DAPI staining identified all the cell nuclei (*blue*). Scale bar, 40 μm.

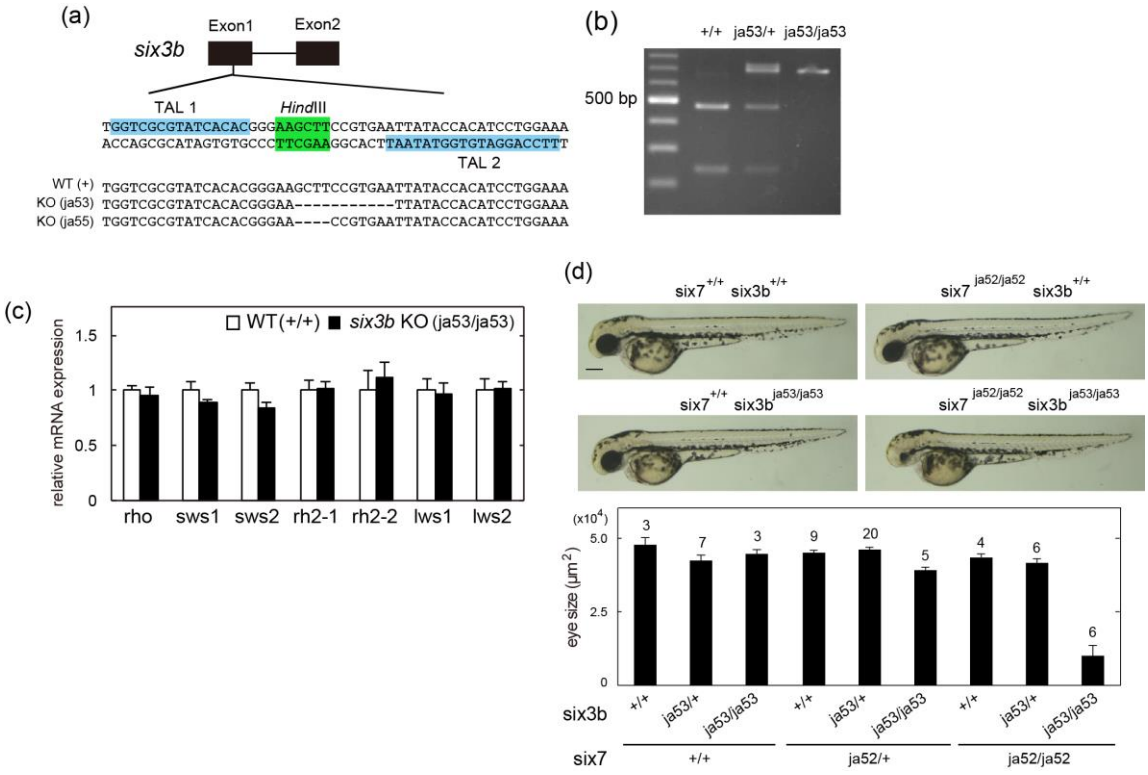

Figure 6. Analysis of *six7* and/or *six3b* knock-out zebrafish larvae. (a) Top, exon-intron organization and partial nucleotide sequences of *six3b* gene in zebrafish. The binding sites of the left and right TALENs are highlighted in *blue*. The recognition site of the endonuclease *Hind*III is highlighted in *green*. Bottom, the nucleotide sequences of the *six3b* knock-out alleles (ja53 and ja55) are compared with the WT sequence. Deletions are showed by dashes. (b) Genotyping of *six3b* knock-out zebrafish by PCR and subsequent digestion by *Hind*III. (c) Expression levels of the opsin genes in the 5-dpf larvae of WT (+/+) and *six3b* knock-out (ja53/ja53). The data are represented by mean + SEM (n = 5). For any members of the phototransduction genes, statistical significance was not obvserved between the WT and *six3b* knock-out zebrafish ($p < 0.05$, Student's *t*-test). (d) Top, images of whole body of the 2-dpf larval zebrafish. To generate the *six3b*/*six7* double knock-out fish and the control fish, the *six3b*-het/*six7*-het double heterozygous fish were crossed with each other and the resultant larvae were raised and used for the analysis. Scale bar, 200 μm. Bottom, the eye area of the mutant fish. The eye area was measured with ImageJ software. The data are represented by mean + SEM. The number of the zebrafish used for the quantification is showed in the bar graph.

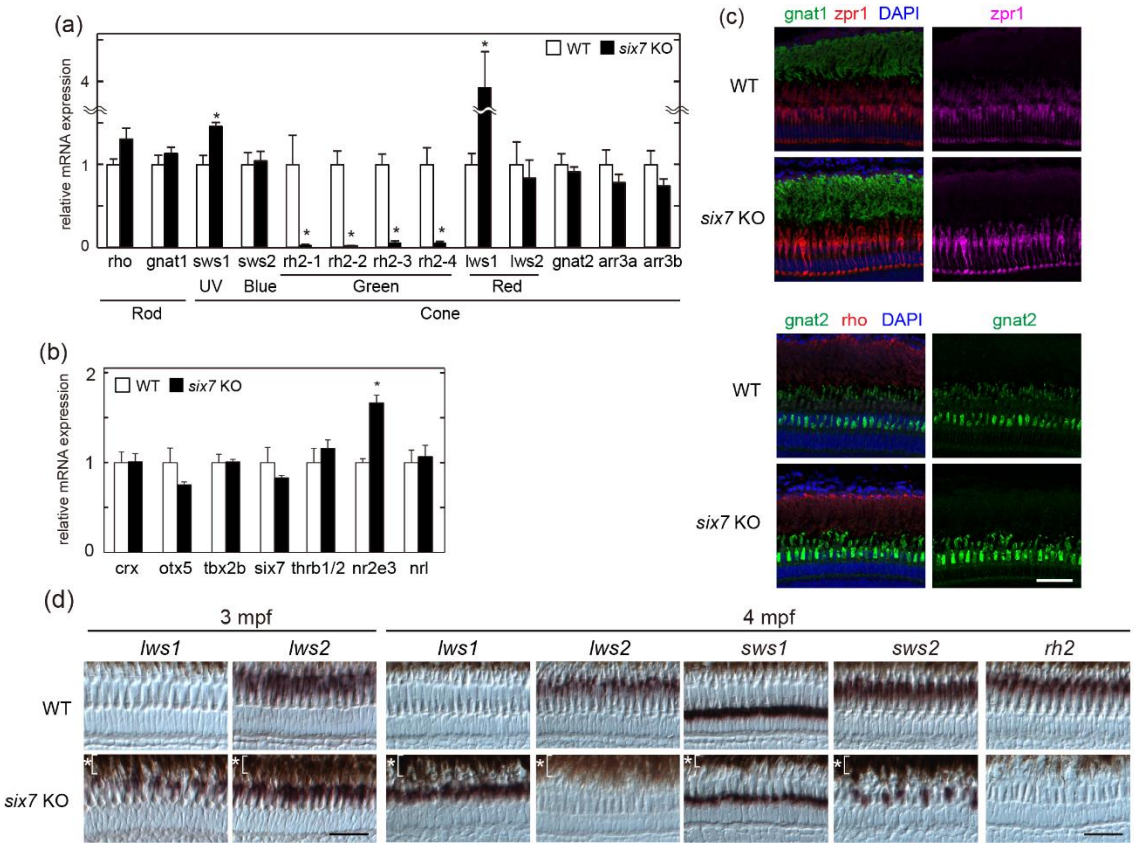

Figure 7. Analysis of the *six7* knock-out zebrafish at the adult stage. (a, b) mRNA levels of phototransduction component genes (a) and transcription factors contributing to the photoreceptor development in mouse and/or zebrafish (b) in the eyes of wild-type (WT) and *six7* knock-out fish at 3 mpf. The RT-qPCR data are indicated by mean + SEM (n = 4). Statistical significance between WT and *six7* knock-out data is shown as the asterisks (*p<0.05 by Student's *t*-test). (c) Immunofluorescent signals in the central retina of the 3-mpf adult WT and KO. The antibodies used were as follows: the anti-Gnat2 antibody for all the cone subtypes (*green*); the anti-rhodopsin antibody for rod cells (*red*). DAPI staining identified all the cell nuclei (*blue*). Scale bar, 40 μm. (d) Expression profiles of cone opsin genes in the central retina of the adult WT and *six7* knock-out by *in situ* hybridization at 3 mpf. For visualizing all the subsets of green cones, I mixed and used four different RNA probes, each of which specifically recognizes the corresponding subtype of the green opsin gene (*rh2-1, rh2-2, rh2-3* and *rh2-4*). RPE is indicated by the asterisks. Scale bars, 30 μm.

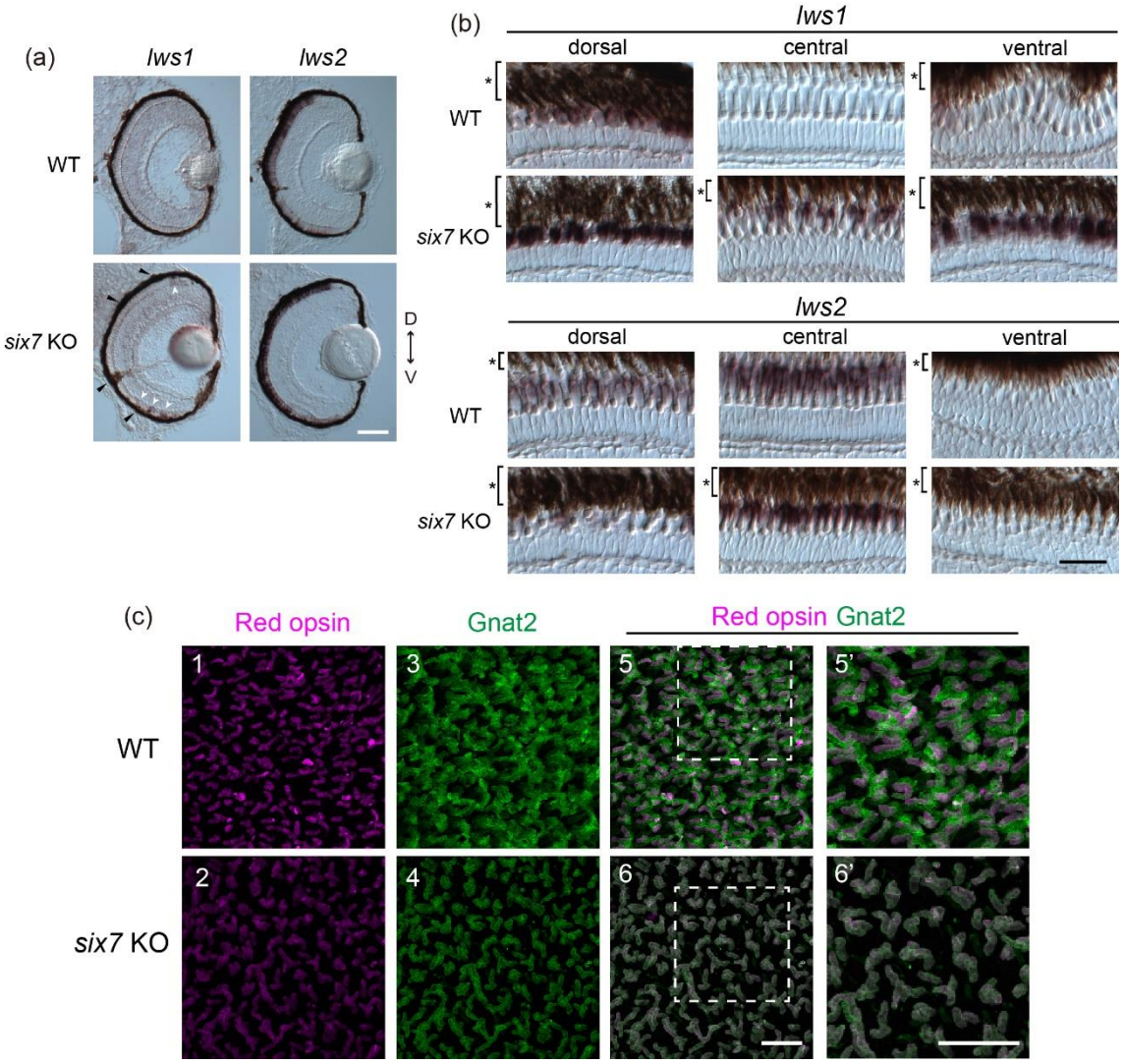

Figure 8. Expression patterns of *lws1* and *lws2* in the retina of WT and *six7* knock-out at both the larval and adult stages. (a, b) The expression patterns of two duplicated red opsin genes, *lws1* and *lws2*, were detected by *in situ* hybridization. (a) Retinal cryosections of the larval zebrafish at 3.5 dpf, which was the same developmental stage as in figure 5c, 5e and 5f. The *lws1*-expressing cell was observed only in *six7* knock-out (arrowheads). The photoreceptor layer is adjacent to the retinal pigment epithelium (RPE, black arrowheads). D, dorsal side. V, ventral side. Scale bar, 50 µm. (b) Related to figure 7d. Retinal cryosections of the adult retina at 3 mpf, which was the same developmental stage as in figure 7a. RPE is indicated by the asterisks. Scale bar, 30 µm. (c) Fluorescent images of the flat-mounted retina of the 6 mpf-WT and *six7* knock-out fish. The antibodies used were as follows: the 1D4 antibody for all the subtypes of the red cones (45) (magenta; panel 1, 2); the anti-Gnat2 antibody for all the subtypes of cones (*green*; panel 3, 4). The fluorescent signals were obtained by focusing on the layer including the outer segment of the double cone in the central retina. Merged images are shown on panel 5 and penal 6, and their magnified images (outlined by a white dotted box in panel 5 and panel 6) are on panel 5' and 6'. Scale bar, 30 µm.

5 年以内に雑誌等で刊行予定のため、非公開。

(a)

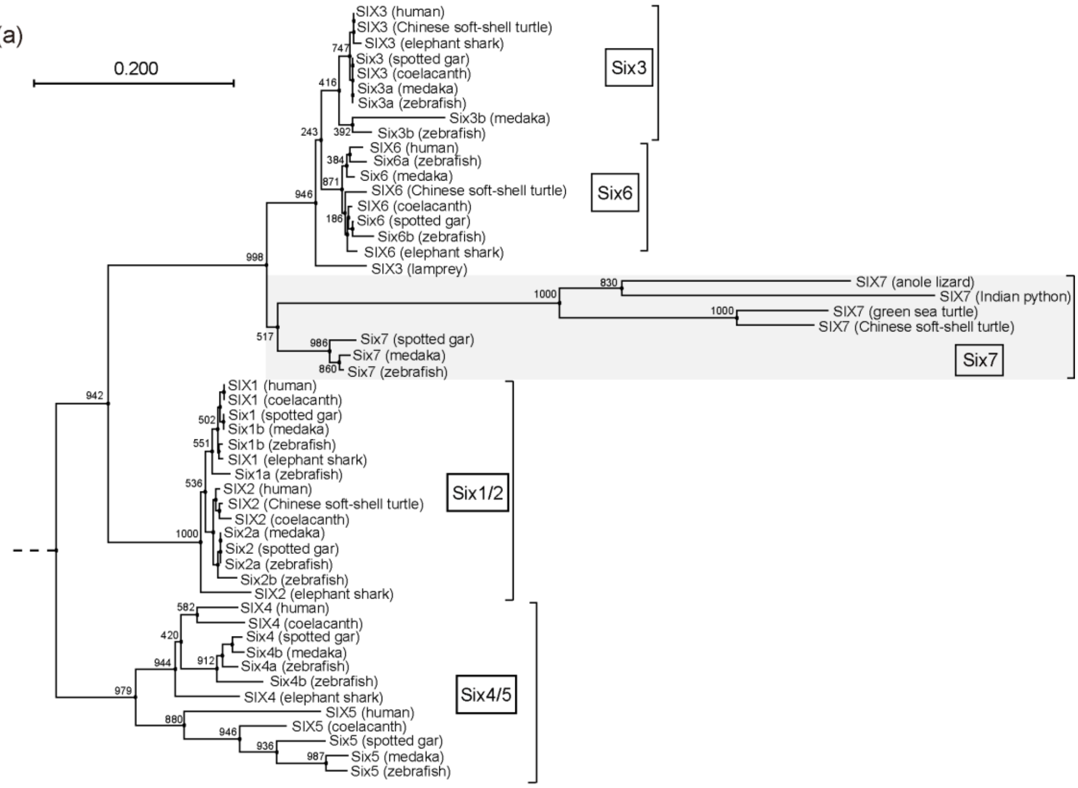
0.200
SIX3 (human)
SIX3 (Chinese soft-shell turtle)
SIX3 (elephant shark)
Six3 (spotted gar)
SIX3 (coelacanth)
Six3a (medaka)
Six3a (zebrafish)
Six3b (medaka)
Six3b (zebrafish)
SIX6 (human)
Six6a (zebrafish)
Six6 (medaka)
SIX6 (Chinese soft-shell turtle)
SIX6 (coelacanth)
Six6 (spotted gar)
Six6b (zebrafish)
SIX6 (elephant shark)
SIX3 (lamprey)
SIX7 (anole lizard)
SIX7 (Indian python)
SIX7 (green sea turtle)
SIX7 (Chinese soft-shell turtle)
Six7 (spotted gar)
Six7 (medaka)
Six7 (zebrafish)
SIX1 (human)
SIX1 (coelacanth)
Six1 (spotted gar)
Six1b (medaka)
Six1b (zebrafish)
SIX1 (elephant shark)
Six1a (zebrafish)
SIX2 (human)
SIX2 (Chinese soft-shell turtle)
SIX2 (coelacanth)
Six2a (medaka)
Six2 (spotted gar)
Six2a (zebrafish)
Six2b (zebrafish)
SIX2 (elephant shark)
SIX4 (human)
SIX4 (coelacanth)
Six4 (spotted gar)
Six4b (medaka)
Six4a (zebrafish)
Six4b (zebrafish)
SIX4 (elephant shark)
SIX5 (human)
SIX5 (coelacanth)
Six5 (spotted gar)
Six5 (medaka)
Six5 (zebrafish)
Six3
Six6
Six7
Six1/2
Six4/5

(b)

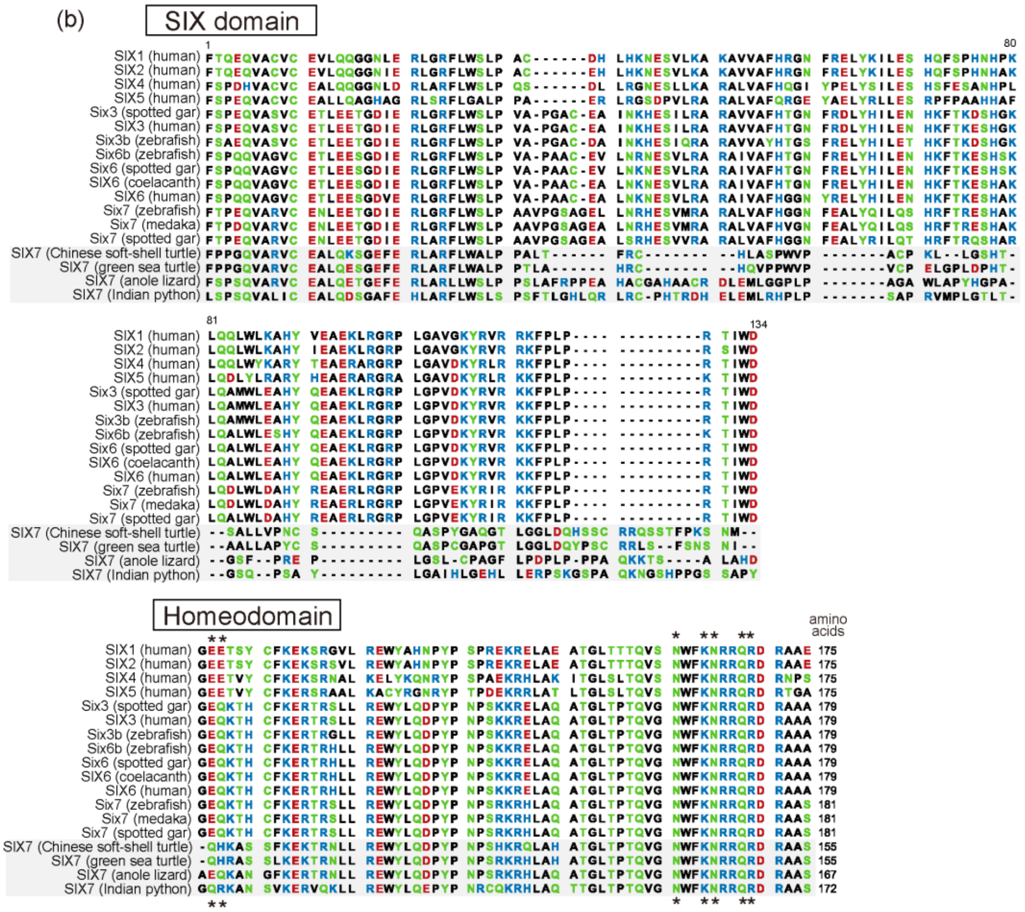
SIX domain
Homeodomain
amino acids

Figure 21. Phylogenetic tree and sequence alignment of the members of vertebrate Six family including reptilian SIX7-like proteins. (a) Phylogenetic tree was constructed from amino acid sequences of SIX domain and homeodomain and generated by using the neighbor-Joining (NJ) method with 1,000 bootstrapping replications. Numerical values are indicated at branch nodes. Nematode CEH-34 was used as an outgroup. The NJ tree includes SIX7-like protein sequences of four reptilian species: Chinese soft-shell turtle (*Pelodiscus sinensis*), anole lizard (*Anolis carolinensis*), green sea turtle (*Chelonia mydas*) and Indian python (*Python molurus*). Scale bar indicates 0.200 substitutions per site. (b) Sequence alignment of Six protein family. Note that the amino acid sequences of the reptilian SIX7-like protein are poorly aligned with all the other members of Six family. The seven residues forming the nucleic acid recognition helix (56) are indicated by the asterisks.

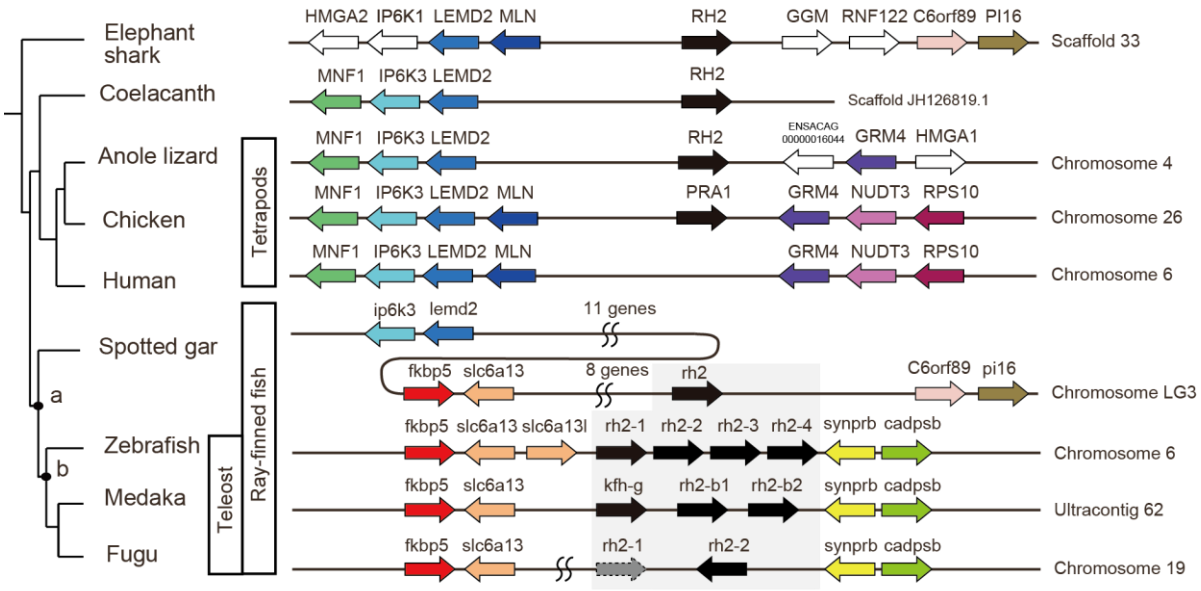

Figure 22. Syntenic regions conserved near to the green cone opsin genes (*rh2*) in vertebrates. Orthologous gene is indicated in the same color. The synteny around the green cone opsin genes (arrows in black) was compared among vertebrate species by using the Ensembl genome browser. See also figure 23 for teleost *rh2* syntenic regions including additional species. The chromosomal locations of the *rh2* green cone opsin genes can be classified into two types, (i) the non-teleost type (top half) and (ii) the teleost type (bottom half). Note that the type (i) synteny is observed in elephant shark, which was diverged at the most ancient period from the other vertebrate species, suggesting that the non-teleost type synteny represents an ancient type. Furthermore, the intermediate-type synteny is observed in spotted gar, which is the closest relative to teleost and retains *six7*. The synteny of spotted gar suggests that the genes around *rh2* was rearranged at least twice during the course of the evolution leading to the teleost (represented by the node “a” and “b”). An incompletely annotated green cone opsin gene is indicated by an arrow in grey. Elephant shark, *Callorhinchus milii*; zebrafish, *Danio rerio*; medaka, *Oryzias latipes*; fugu, *Takifugu rubripes*; spotted gar, *Lepisosteus oculatus*; coelacanth, *Latimeria chalumnae*; anole lizard, *Anolis carolinensis*; chicken, *Gallus gallus*; human, *Homo sapiens*.

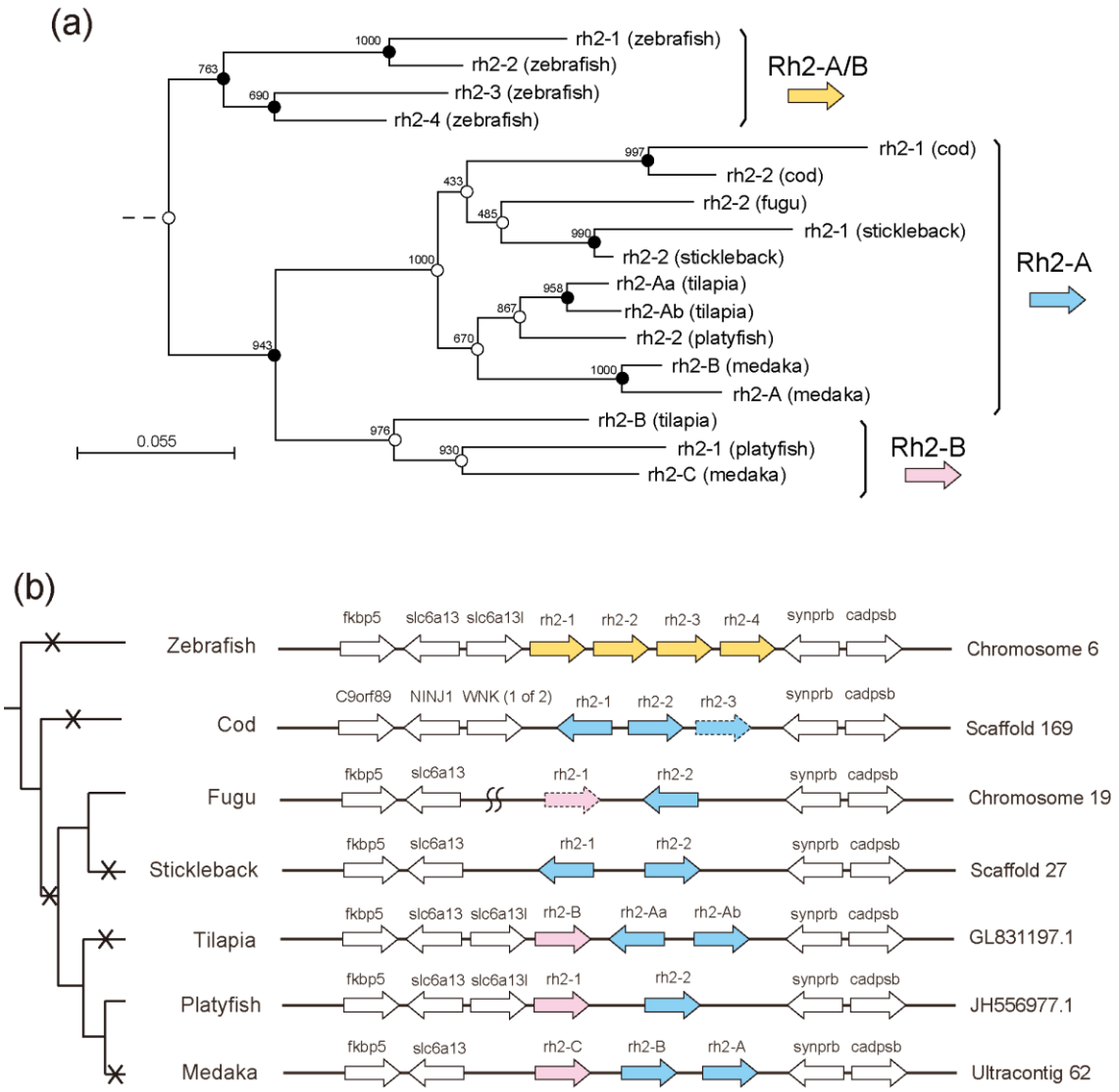
(a)
rh2-1 (zebrafish)
rh2-2 (zebrafish)
rh2-3 (zebrafish)
rh2-4 (zebrafish)
Rh2-A/B
rh2-1 (cod)
rh2-2 (cod)
rh2-2 (fugu)
rh2-1 (stickleback)
rh2-2 (stickleback)
rh2-Aa (tilapia)
rh2-Ab (tilapia)
rh2-2 (platyfish)
rh2-B (medaka)
rh2-A (medaka)
Rh2-A
rh2-B (tilapia)
rh2-1 (platyfish)
rh2-C (medaka)
Rh2-B
0.055
1000
763
690
997
433
485
990
1000
958
867
670
1000
943
976
930
(b)
Zebrafish
fkbp5 slc6a13 slc6a13l rh2-1 rh2-2 rh2-3 rh2-4 synprb cadpsb
Chromosome 6
Cod
C9orf89 NINJ1 WNK (1 of 2) rh2-1 rh2-2 rh2-3 synprb cadpsb
Scaffold 169
Fugu
fkbp5 slc6a13 rh2-1 rh2-2 synprb cadpsb
Chromosome 19
Stickleback
fkbp5 slc6a13 rh2-1 rh2-2 synprb cadpsb
Scaffold 27
Tilapia
fkbp5 slc6a13 slc6a13l rh2-B rh2-Aa rh2-Ab synprb cadpsb
GL831197.1
Platyfish
fkbp5 slc6a13 slc6a13l rh2-1 rh2-2 synprb cadpsb
JH556977.1
Medaka
fkbp5 slc6a13 rh2-C rh2-B rh2-A synprb cadpsb
Ultracontig 62

Figure 23. Phylogenetic tree of the members in teleost green cone opsins and syntenic regions conserved near to the green cone opsin genes in teleost. (a) A phylogenetic tree was constructed from the amino acid sequences of the green cone opsins without N terminal and C terminal regions and generated by using the Neighbor-Joining method with 1,000 bootstrapping replications. Numerical values are indicated at branch nodes. The intraspecific (*closed*) and interspecific (*open*) duplication of green opsin genes were represented as closed and open circles on the nodes. Spotted gar Rh2 was used as an outgroup. The scale bar indicates the number of amino acid substitutions per site. Teleost Rh2 was separated into three groups: Rh2-A/B, Rh2-A and Rh2-B. (b) Chromosomal locations of the green opsin genes were compared among teleost species. Three groups of green opsin genes [see the phylogenetic tree (a)] are indicated with different colors: *yellow* for Rh2-A/B, *blue* for Rh2-A, and *pink* for Rh2-B. Incompletely annotated green opsin genes are indicated by arrows surrounded by a broken line. The local duplication of the green opsin genes is represented as a cross mark in the phylogeny. Zebrafish, *Danio rerio*; medaka, *Oryzias latipes*; cod, *Gadus morhua*; fugu, *Takifugu rubripes*; stickleback, *Gasterosteus aculeatus*; tilapia, *Oreochromis niloticus*; platyfish, *Xiphophorus maculatus.*

5 年以内に雑誌等で刊行予定のため、非公開。

8. Acknowledgement

I thank members of Fukada lab for valuable discussion. In particular, I appreciate Dr. Yoshitaka Fukada, Dr. Daisuke Kojima, Dr. Tomoya Shiraki and Dr. Kimiko Shimizu for teaching and encouraging me at any times. I thank to National BioResource Project, Zebrafish, Core Institution (NZC) for providing the transgenic lines. I also thank Dr. Shoji Kawamura for zebrafish cone opsin transgenic lines. I also thank Dr. Shigehiro Kuraku (RIKEN) for valuable comments. I am grateful to members of FACS core laboratory, the University of Tokyo, for support of cell sorting.

I thank Mr. Koyo Ogawa and Ms. Setsuko Ogawa, my parents, for taking very much care of me and for financial and mental support. I owe what I am entirely to members of my family and to my friends. Thanks a lot!!